



LUND UNIVERSITY

Mechanisms of Shiga toxin-mediated signaling and toxicity

Johansson, Karl

2020

Document Version:

Publisher's PDF, also known as Version of record

[Link to publication](#)

Citation for published version (APA):

Johansson, K. (2020). *Mechanisms of Shiga toxin-mediated signaling and toxicity*. [Doctoral Thesis (compilation), Department of Clinical Sciences, Lund]. Lund University, Faculty of Medicine.

Total number of authors:

1

General rights

Unless other specific re-use rights are stated the following general rights apply:

Copyright and moral rights for the publications made accessible in the public portal are retained by the authors and/or other copyright owners and it is a condition of accessing publications that users recognise and abide by the legal requirements associated with these rights.

- Users may download and print one copy of any publication from the public portal for the purpose of private study or research.
- You may not further distribute the material or use it for any profit-making activity or commercial gain
- You may freely distribute the URL identifying the publication in the public portal

Read more about Creative commons licenses: <https://creativecommons.org/licenses/>

Take down policy

If you believe that this document breaches copyright please contact us providing details, and we will remove access to the work immediately and investigate your claim.

LUND UNIVERSITY

PO Box 117
221 00 Lund
+46 46-222 00 00

OPEN

Shiga toxin signals via ATP and its effect is blocked by purinergic receptor antagonism

Karl E. Johansson¹, Anne-Lie Ståhl¹, Ida Arvidsson¹, Sebastian Loos¹, Ashmita Tontanahal¹, Johan Rebetz¹, Milan Chromek¹, Ann-Charlotte Kristoffersson¹, Ludger Johannes² & Diana Karpman¹

Shiga toxin (Stx) is the main virulence factor of enterohemorrhagic *Escherichia coli* (EHEC), that cause gastrointestinal infection leading to hemolytic uremic syndrome. The aim of this study was to investigate if Stx signals via ATP and if blockade of purinergic receptors could be protective. Stx induced ATP release from HeLa cells and in a mouse model. Toxin induced rapid calcium influx into HeLa cells, as well as platelets, and a P2X1 receptor antagonist, NF449, abolished this effect. Likewise, the P2X antagonist suramin blocked calcium influx in HeLa cells. NF449 did not affect toxin intracellular retrograde transport, however, cells pre-treated with NF449 exhibited significantly higher viability after exposure to Stx for 24 hours, compared to untreated cells. NF449 protected HeLa cells from protein synthesis inhibition and from Stx-induced apoptosis, assayed by caspase 3/7 activity. The latter effect was confirmed by P2X1 receptor silencing. Stx induced the release of toxin-positive HeLa cell- and platelet-derived microvesicles, detected by flow cytometry, an effect significantly reduced by NF449 or suramin. Suramin decreased microvesicle levels in mice injected with Stx or inoculated with Stx-producing EHEC. Taken together, we describe a novel mechanism of Stx-mediated cellular injury associated with ATP signaling and inhibited by P2X receptor blockade.

Shiga toxin (Stx) is the main virulence factor of enterohemorrhagic *Escherichia coli* (EHEC). These strains are causally associated with hemolytic uremic syndrome (HUS), a major cause of acute renal failure. There are two major variants of Stxs, Stx1 and Stx2, that are approximately 60% homologous¹. The toxin consists of one enzymatically active A-subunit and a pentameric B-subunit^{2,3}. The Stx B-subunit binds to the glycolipid receptor globotriaosylceramide (Gb3) or globotetraosylceramide (Gb4)⁴, leading to internalization of the toxin⁵. Once endocytosed, Stx undergoes retrograde transport via the Golgi apparatus to the endoplasmic reticulum. During retrograde transport the A-subunit is cleaved by furin into A₁ and A₂ fragments⁶. From the ER the A₁ fragment is released into the cytosol where it depurinates an adenine base from the 28S rRNA of the ribosome³, thereby inhibiting protein synthesis and subsequently leading to cell death^{7,8}. Stx induces apoptosis in intestinal⁹ and kidney¹⁰ cells *in vivo* and also in HeLa cells *in vitro*¹¹.

Upon receptor binding, Stx1 and Stx2 can trigger cellular activation and host responses (reviewed in^{12,13}). Stx1 has been shown to induce calcium influx into HeLa cells¹⁴. Furthermore, Stx2 stimulates microvesicle shedding from activated blood cells^{15–18}. Microvesicles are extracellular vesicles, shed directly from the plasma membrane¹⁹. Their formation is a regulated process initiated by elevation in intracellular calcium levels leading to loss of plasma membrane lipid asymmetry and cleavage of cortical actin²⁰. Microvesicles act as carriers of proteins, lipids and nucleic acids, delivering their cargo to target cells²¹. Importantly, in the context of Stx-mediated HUS, microvesicles transfer the toxin to the kidney¹⁶.

Purinergic receptors are a family of trans-membrane receptors sub-divided into P1 and P2 receptors, based on ligand binding. P1 receptors are activated by adenosine and P2 receptors are activated by ATP and other purine nucleotides²². P2 receptors are further subdivided into ionotropic P2X and metabotropic P2Y receptors²³ and the P2X1 receptor is a known calcium channel in platelets²⁴.

Here we investigated if Stx-induces cellular activation and damage via ATP signaling and, if so, if injury could be decreased by blockade of purinergic signaling. To this end, we used HeLa cells and platelets incubated with

¹Department of Pediatrics, Clinical Sciences Lund, Lund University, Lund, Sweden. ²Institut Curie, U1143 INSERM, UMR3666 CNRS, Cellular and Chemical Biology unit, Paris, France. Correspondence and requests for materials should be addressed to D.K. (email: diana.karpman@med.lu.se)

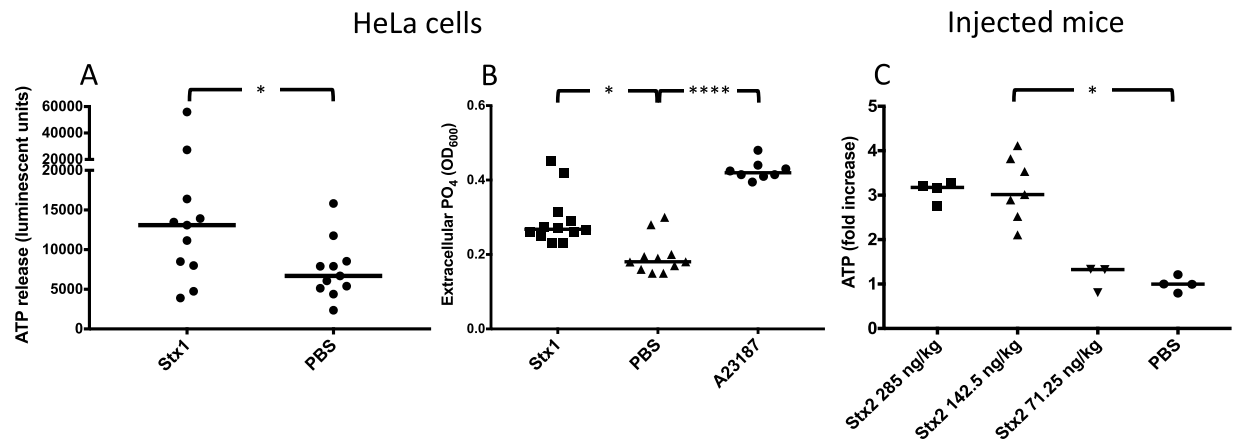


Figure 1. Shiga toxin induces release of ATP *in vitro* and *in vivo*. **(A)** HeLa cells ($n = 11$) were stimulated with Shiga toxin 1 (Stx1) or PBS and the ATP content was measured after 5 min. The median extracellular ATP content is depicted as the bars. **(B)** HeLa cells were stimulated with Stx1 ($n = 12$), A23187 calcium ionophore ($n = 8$) or PBS ($n = 11$). The supernatant was collected and free phosphate groups were measured. Data is depicted as median absorbance at OD₆₀₀ (denoted by the bars), correlating to free phosphate groups in the supernatant. **(C)** Mice were injected with Stx2 at a concentration of 285 ($n = 4$), 142.5 ($n = 7$) or 71.25 ng/kg ($n = 3$) or with PBS as the control. Mice injected with Stx2 142.5 ng/kg had significantly higher plasma ATP levels compared to PBS control mice. A similar trend was seen for mice injected with Stx2 285 ng/kg, although the difference did not achieve statistical significance. Mice injected with Stx2 71.25 ng/kg had plasma ATP levels comparable to PBS control mice. The median is denoted by the bar. * $P < 0.05$, **** $P < 0.0001$, two-tailed Mann-Whitney test (panel A) and Kruskal-Wallis test (panels B and C).

the P2X1 specific antagonist NF449²⁵ and the non-selective P2X antagonist suramin²⁶ and P2X1-deficient HeLa cells, to determine the effect of purinergic signaling on Stx-mediated calcium influx, toxin retrograde transport, cytotoxicity and microvesicle release. We used an established mouse model^{27,28}, in which mice were injected with Stx, to study ATP release, and investigated the effect of purinergic receptor blockade on microvesicle shedding in mice injected with Stx2 or inoculated with Stx2-producing *E. coli*.

Results

Stx induced release of ATP *in vitro* and *in vivo*. HeLa cells were stimulated with Stx1 (1 $\mu\text{g}/\text{mL}$). These cells were chosen because they possess the toxin receptor Gb3 and are susceptible to the toxin^{14,29}. ATP was released from HeLa cells stimulated with Stx1 for 5 min. A significant increase in extracellular ATP was detected in the medium of toxin-stimulated cells compared to the phosphate buffered saline (PBS) control (Fig. 1A). The rapid ATP release induced by Stx1 indicated that toxin binding in itself led to the response. A lower concentration of Stx1 (200 ng/mL) also induced the release of extracellular ATP that reached significance after 10 min incubation (Supplementary Fig. S1A). A similar trend, albeit non-significant, was noted when cells were stimulated with Stx2 (1 $\mu\text{g}/\text{mL}$) (Supplementary Fig. S1B). The positive control, histamine, led to rapid ATP release (median 33240 luminescent units).

Free extracellular phosphate groups served as an indicator of ATP degradation after release. A significant increase in phosphate groups was observed in the medium from Stx1-stimulated cells and calcium-ionophore stimulated cells (the positive control) compared to the PBS negative control after 40 min (Fig. 1B), indicating ATP degradation. The data suggest that Stx1 released ATP from HeLa cells and that the signal was degraded extracellularly.

ATP content was analyzed in plasma samples from mice that had been injected with varying doses of Stx2 and sacrificed when symptoms developed. Stx2 was chosen for *in vivo* experiments as its toxicity in murine disease has been previously demonstrated²⁷. Mice treated with Stx2 at a dose of 285 ng/kg developed symptoms on day 3 after injection, those treated with Stx2 142.5 ng/kg developed symptoms on day 4 or 5 and mice treated with the lowest dose (71.25 ng/kg) remained asymptomatic. Plasma ATP was significantly higher in symptomatic toxin-injected mice (Stx2 142.5 ng/kg, Fig. 1C). Mice treated with the lowest dose of Stx2 had ATP levels comparable to untreated mice.

P2X1 receptor antagonist inhibited Stx1 and Stx2-induced calcium influx. To evaluate the importance of Stx-induced ATP-release for Stx1-mediated signaling, experiments were carried out to study if the P2X1 antagonist NF449, or the non-selective P2X inhibitor suramin, could block calcium influx induced by Stx1. HeLa cells loaded with Fluo-4 calcium indicator dye and stimulated with Stx1 displayed a swift and steady increase in cytosolic calcium, lasting for the duration of the experiment, 270 sec (Fig. 2A). NF449- and suramin-pretreated cells exhibited significantly less calcium influx after Stx1 stimulation compared to untreated cells, remaining at stable low calcium concentration levels throughout the experiment (Fig. 2A) as did the HBSS negative control. As a positive control, NF449 treated and untreated HeLa cells were stimulated with ATP. ATP induced a clear calcium response in HeLa cells, while NF449 treated cells were unaffected (Supplementary Fig. S2).

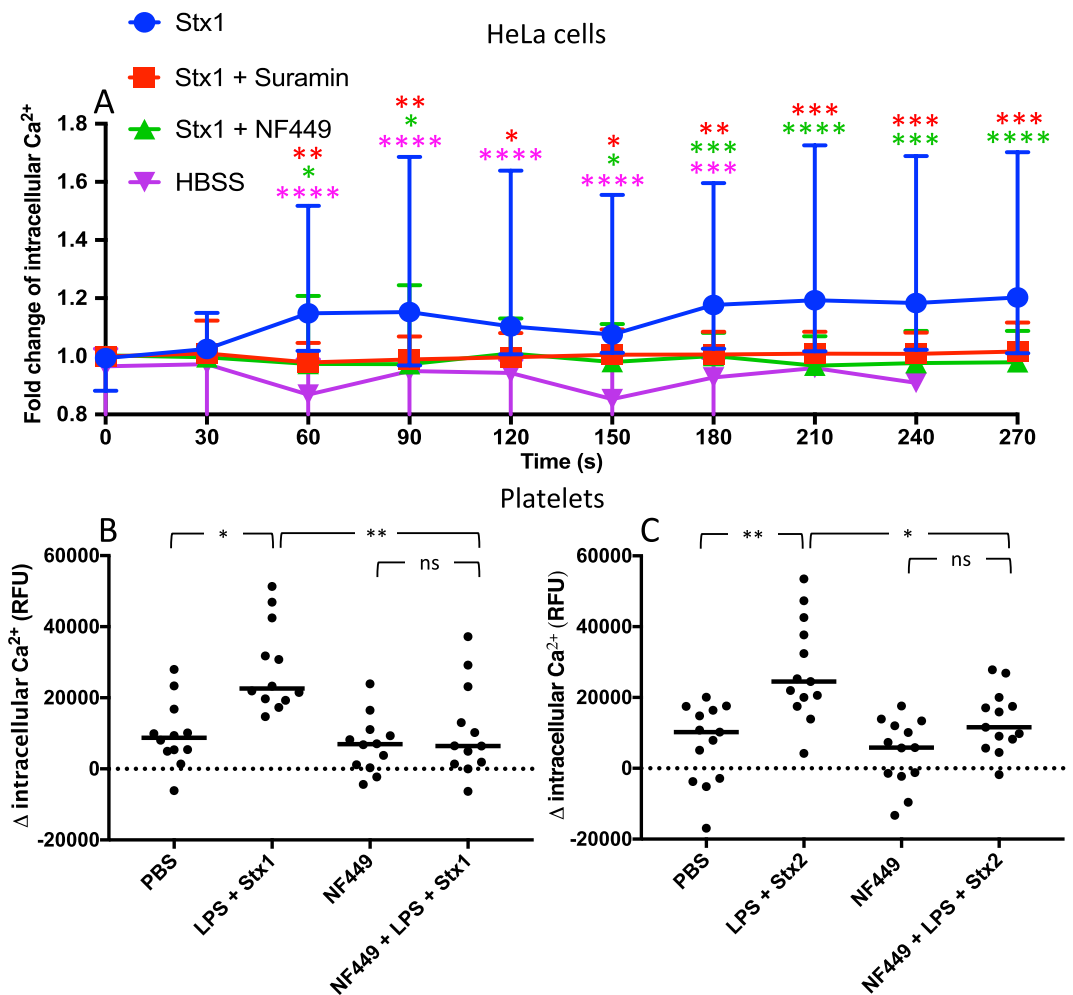


Figure 2. The effect of purinergic antagonists on calcium influx induced by Shiga toxin in HeLa cells and human platelets. **(A)** Calcium influx was measured in HeLa cells preincubated with NF449, suramin or phosphate buffered saline (PBS) vehicle, stimulated with Shiga toxin 1 (Stx1) or Hank's balanced salt solution (HBSS) (groups differentiated by icon colors) and imaged by fluorescence microscopy. Results are presented as mean fluorescent change of all cells in the field of view (median and range). The color of the asterisks corresponds to the color of the icon in comparison to Stx1. The absence of asterisks indicates that statistics was not significant. **(B-C)** Human platelets ($n = 3$ donors) were preincubated with NF449 or PBS vehicle followed by Stx1 (**B**) or Stx2 (**C**) and O157LPS (to enable platelet activation by Shiga toxin) or PBS vehicle. Data is presented as the initial fluorescence subtracted from fluorescence after 2 minutes and the bar denotes the median fluorescence. RFU: relative fluorescent units, ns: not significant, * $P < 0.05$, ** $P < 0.01$, *** $P < 0.001$, **** $P < 0.0001$, two-way repeated measure ANOVA (panel A) and Kruskal-Wallis test (panels B and C).

A similar experiment was carried out using human platelets stimulated with Stx1 or Stx2, together with *E. coli* O157 lipopolysaccharide (LPS) to stimulate platelet activation^{18,30}. An increase in intracellular calcium levels was noted upon Stx1 (Fig. 2B) and Stx2 (Fig. 2C) stimulation. When the cells were pre-treated with NF449 calcium influx was not detected (Fig. 2B,2C). Stx1, Stx2 or O157LPS alone did not have a significant effect on the influx of calcium (Supplementary Fig. S3A,B).

Stx1 localization to the ER was not affected by the P2X1 receptor antagonist. The effect of the P2X1 receptor antagonist NF449 on Stx1-retrograde transport was studied using HeLa cells expressing a SNAP-tag localized to the ER that were incubated with Stx1B labeled with the binding substance O⁶-benzylguanine. NF449 did not affect retrograde trafficking of the toxin to the ER whereas the positive control, the Ca²⁺ chelator BAPTA-AM, resulted in significantly less toxin locating to the ER (Fig. 3).

P2X1 receptor antagonist protected HeLa cells from the cytotoxic effects of Stx. Stx1- and Stx2-treated HeLa cells exhibited considerable cell death, a median of 10.8% (range 2.7–21.3%) and 10.1% (range 6.8–25.9%), respectively, were viable after 24 h. Cell viability was significantly higher in cells that were pre-treated with NF449 with a median of 72.3% (range 63.9–97.9%) for Stx1 and 62.4% (34.9–109.6%) for Stx2 compared to PBS-treated cells, defined as 100% viability (Fig. 4A).

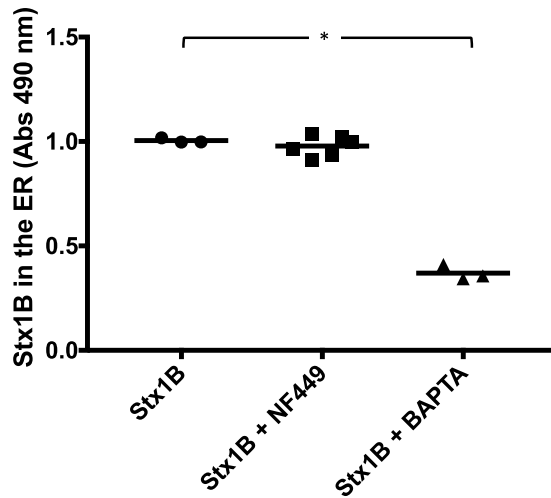


Figure 3. The effect of NF449 on retrograde transport of Shiga toxin 1B. HeLa cells transfected with the ER-anchored SNAP-tag were treated with NF449 (n = 6), the Ca²⁺ chelator BAPTA-AM (n = 3) or PBS vehicle (n = 3) followed by Shiga toxin (Stx) 1B-subunit:O⁶-benzylguanidine. No difference in Stx1B localization to the ER could be seen between NF449-treated and PBS-treated cells. Data is shown as median absorbance values (OD₄₉₀) from SNAP-captured Stx1B. The median is depicted by the bar. *P < 0.05, n.s.: non-significant, Kruskal-Wallis test.

P2X1 receptor antagonist partially protected HeLa cells from Stx1-mediated ribotoxicity. The effect of Stx1 on protein synthesis was investigated in the presence of NF449. HeLa cells incubated with Stx1 alone for 4 h displayed a median of 28% (range 13–49%) protein synthesis compared to unstimulated control cells (defined as 100%). Pre-incubation with NF449 increased protein synthesis to 37% (range 27–56%) compared to unstimulated cells (Fig. 4B).

P2X1 receptor antagonist reduced Stx1-induced caspase 3/7 activation. Stx1 was incubated with HeLa cells for 24 h and induced caspase 3/7 activation in a majority of the cells, suggesting the induction of apoptotic signals (Fig. 4C). Pretreatment with NF449 lead to significantly less caspase 3/7 activation per cell (Fig. 4C). Similar results were obtained with Stx2 (Supplementary Fig. S4).

Cells with reduced P2X1 receptor expression, due to silencing, displayed significantly lower caspase-3/7 activation in response to Stx1 compared to control cells transfected with a scrambled sequence (Fig. 4D), supporting involvement of the receptor. PBS-treated native (n = 3) and P2X1-silenced HeLa cells (n = 2) did not display caspase 3/7-activation (data not shown).

P2X receptor antagonists decreased the release of Stx1 and Stx2-positive microvesicles.

Calcium influx induces microvesicle release³¹ and, as shown above, Stx triggers calcium influx, which has also been demonstrated for Stx1B¹⁴. Stx1B stimulation induced microvesicle release from HeLa cells that was reduced in the presence of NF449, although this did not achieve statistical significance (Fig. 5A). HeLa cell-derived microvesicles containing Stx1B were significantly reduced in the presence of NF449 (Fig. 5B). Experiments were also carried out in whole blood in which Stx1 (holotoxin) induced a significant release of microvesicles from platelets (Fig. 5C) and NF449 significantly reduced the release of Stx1-positive platelet microvesicles (Fig. 5D). Similar experiments were carried out with Stx2 (holotoxin). Stx2 stimulation induced the release of HeLa cell microvesicles, an effect that was significantly reduced by NF449 (Fig. 5E). Likewise, the release of toxin-positive microvesicles was significantly decreased by NF449 (Fig. 5F). Platelet-derived microvesicles were released in whole blood stimulated with Stx2 (Fig. 5G), this effect was significantly reduced by suramin (Supplementary Fig. S5) and by NF449, albeit without achieving significance (Fig. 5G). Significantly less Stx2-positive platelet microvesicles were released in the presence of NF449 (Fig. 5H).

Suramin inhibits Stx2-induced platelet-derived microvesicle release *in vivo* in a Stx2 and EHEC mouse model. The effect of suramin treatment on platelet-derived microvesicles, and the release of Stx2-positive microvesicles, was assessed in BALB/c mice injected with Stx2. Suramin was chosen for the *in vivo* studies due to its non-selective antagonistic properties with regard to P2X receptors³². Levels of platelet-derived microvesicles were significantly higher in mice injected with Stx2 compared to controls (Fig. 6A). Platelet-derived microvesicles and those that were Stx2-positive were significantly lower in suramin-treated mice (Fig. 6A,B).

The effect of suramin treatment was assessed in BALB/c mice infected with Stx2-producing *E. coli* O157:H7. The number of total platelet-derived microvesicles, and those that were Stx2-positive, in plasma from mice infected with *E. coli* O157:H7 was significantly higher compared to the control mice (inoculated with vehicle) and suramin treatment significantly reduced this effect (Fig. 6C,D).

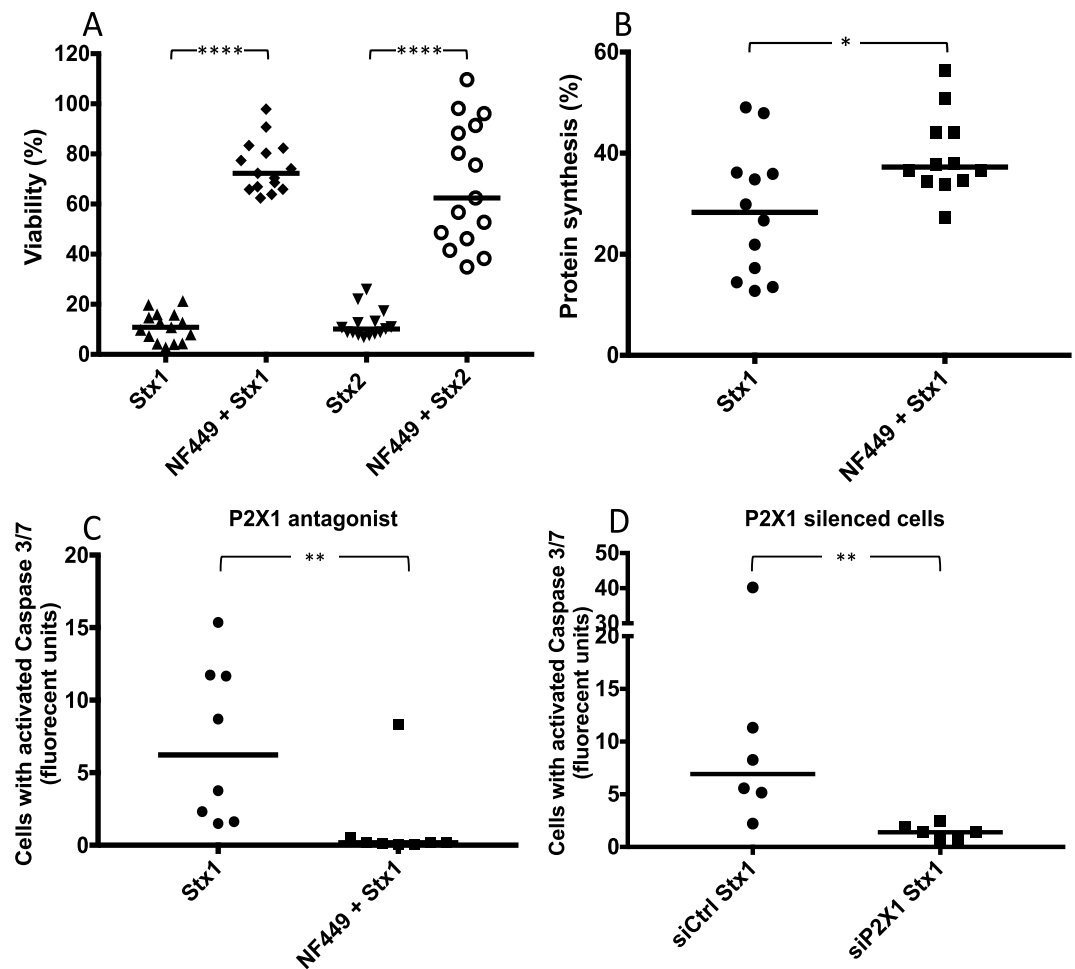


Figure 4. The effect of NF449 on HeLa cell viability upon Shiga toxin intoxication. (A) PBS-treated and NF449-treated HeLa cells were incubated with Shiga toxin (Stx)1 or Stx2 for 24h. NF449-treated cells exhibited 61.5% and 52.3% less cell death compared to PBS-treated cells (defined as 100%) when challenged with Stx1 and Stx2, respectively. Median viability is depicted by the bar. (B) HeLa cells treated with NF449 or PBS vehicle were incubated with Stx1 and protein synthesis was measured. PBS-treated cells displayed a lower protein synthesis (median 28%) compared to cells pretreated with NF449 (median 37%). Protein synthesis is presented as percent ^{35}S divided by total protein content compared to the toxin-free control (defined as 100%). The median protein synthesis is depicted as the bar. (C) Stx1-induced caspase 3/7 activation was measured in HeLa cells pretreated with NF449 or left untreated, showing less caspase 3/7 activation in the cells that were pretreated with NF449. (D) HeLa cells were transfected with siP2X1 or siCtrl ($n = 6$) and challenged with Stx1, showing less caspase 3/7 activation in cells transfected with siP2X1. Median caspase 3/7 activation per cell is denoted by the bar. * $P < 0.05$, ** $P < 0.01$, **** $P < 0.0001$, two-tailed Mann-Whitney test.

Discussion

Stx, the major virulence factor of EHEC strains, causes massive intestinal and renal cellular damage. This study demonstrates a novel mechanism by which Stx activates and damages cells. Stx induces a cellular signal promoting the release of ATP followed by ATP signaling via purinergic receptors, leading to calcium influx into cells associated with toxin-associated cellular damage and microvesicle release. Stx mediates cellular injury by binding to the Gb3 receptor and undergoing cellular uptake, retrograde transport and thereafter causing cell death by inhibition of protein synthesis and induction of apoptosis. The toxin gains access to the circulation, binds to blood cells and induces the release of blood cell-derived microvesicles³³. Stx reaches the kidney bound to the cell membrane of blood cells or within blood cell-derived microvesicles¹⁶. This study shows that ATP signaling is involved in fundamental aspects of Stx-mediated cellular effects as depicted in Fig. 7. This novel ATP-mediated effect of Stx was inhibited by the P2X1 antagonist NF449, and the non-selective antagonist suramin. NF449 blocked toxin-associated calcium influx and reduced cytotoxicity, associated with inhibited protein synthesis and caspase activity, as well as microvesicle release. The latter effect, on microvesicle release, was confirmed in two *in vivo* models using Stx2 injection and *E. coli* O157 inoculation. Purinergic antagonism could thus block crucial aspects of Stx-induced cellular activation and injury. The findings suggest that ATP signaling can promote the cellular effects of Stx and that blocking purinergic receptors may have a protective effect.

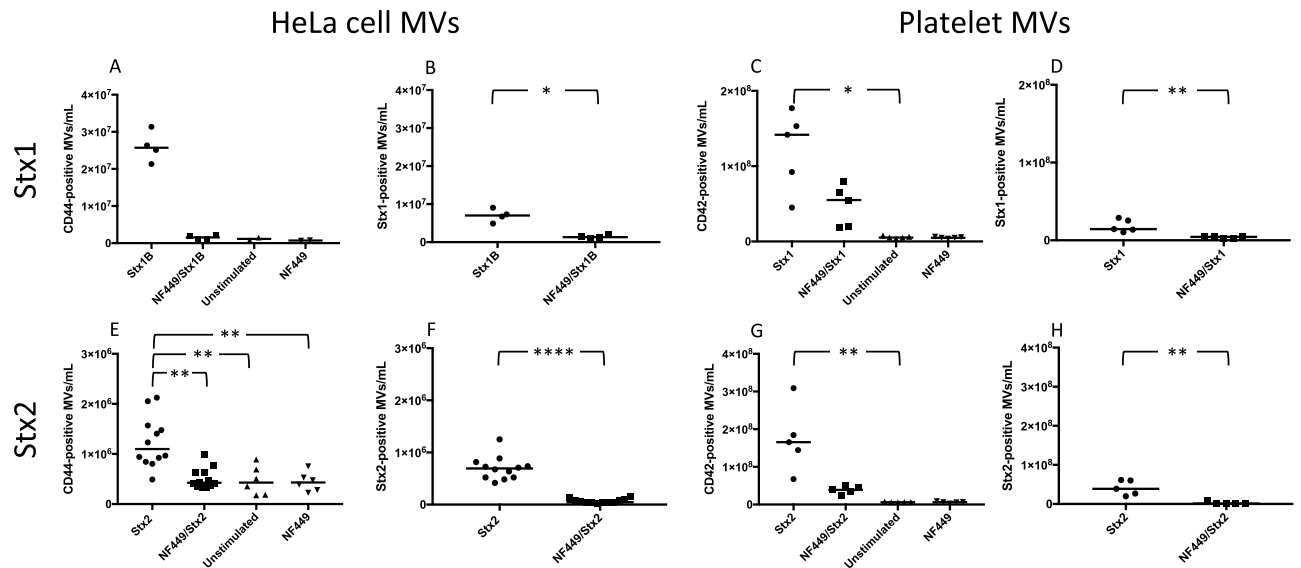


Figure 5. NF449 inhibits the release of toxin-positive microvesicles from HeLa cells and platelets. (A–B) HeLa cells were pretreated NF449 or left untreated and stimulated with Shiga toxin 1B (Stx1B). Microvesicle release was measured by flow cytometry. (A) Stx1B induced the release of microvesicles from HeLa cells (CD44 +), the effect was not significant compared to NF449 pretreated cells (median microvesicles (MV) in NF449 control was 7.3×10^5 /mL). (B) The release of toxin-positive microvesicles (those containing Stx1B) was significantly decreased by NF449 (median MVs in NF449/Stx1B was 1.3×10^6 /mL). (C–D) Whole blood was pretreated with NF449 or left untreated and stimulated with Stx1 (holotoxin). (C) Stx1 induced a significant release of platelet-derived microvesicles (CD42 +, median MVs in NF449 control was 4.8×10^6 /mL). (D) The release of toxin-positive platelet microvesicles was significantly reduced in the presence of NF449 (median MVs in NF449/Stx1 was 4.4×10^6 /mL). (E–F) HeLa cells were pretreated with NF449 or left untreated and stimulated with Stx2 (holotoxin). (E) Stx2 induced a significant release of microvesicles that was significantly reduced by NF449 (median MVs in NF449 control was 3.8×10^5 /mL). (F) Toxin-positive microvesicle release was significantly reduced by NF449 (median MVs in NF449/Stx2 was 4.7×10^4 /mL). (G–H) Whole blood was pretreated with NF449 or left untreated and stimulated with Stx2. (G) Stx2 induced a significant release of platelet-derived microvesicles (median MVs in unstimulated control was 6.3×10^6 /mL). (H) NF449 significantly reduced the release of Stx2-positive microvesicles from platelets (median MVs in NF449/stx2 was 1×10^6 /mL). Median microvesicles/mL is denoted as the bar. * $P < 0.05$, ** $P < 0.01$, *** $P < 0.0001$, two-tailed Mann-Whitney test (panels B, D, F and H) and Kruskal-Wallis test (panels A, C, E and G).

Stx1 induces calcium influx¹⁴. The mechanism by which the toxin induces calcium influx has not been previously elucidated. Here we show that toxin induces ATP efflux, which then binds to and activates the P2X1 receptor triggering calcium influx that could be demonstrated for both Stx1 and Stx2. The effect of Stx2 was specifically assayed in the presence of apyrase, in order to catalyze the hydrolysis of preformed ATP to ADP and AMP and thereby reduce P2X1 desensitization³⁴. This effect of Stx was totally abrogated by the P2X1 receptor antagonist NF449 in HeLa cells (for Stx1) and in platelets (for Stx1 and Stx2). We used HeLa cells throughout the study to obtain reproducible results not dependent on variations between donors and showed that the cells express the P2X1 receptor. We chose to show the effect of Stx1 and Stx2 on ATP signaling even in platelets as these cells are known to express P2X1³⁵ and signaling via the P2X1 receptor was shown to induce calcium influx in platelets (reviewed in²⁴). Moreover, once Stx gains access to the bloodstream it binds to platelets¹⁸, thus the signaling induced in platelets, and its abrogation by NF449, may have relevance in the clinical disease setting.

Blocked ATP signaling and calcium influx affected the ultimate cellular effects of Stx1, i.e. the induction of cell death by inhibited protein translation and apoptosis. These effects were reduced in the presence of the P2X1 receptor antagonist NF449. Calcium flux has been implicated in the induction of apoptosis (reviewed in³⁶). Ribosome-inactivating proteins, such as ricin and Stx, of plant or microbial origin, respectively, require intracellular calcium to induce apoptosis³⁷. Calcium transfer from the ER to mitochondria induced by Stx1, leading to release of cytochrome *c*, activation of caspase-9 and production of reactive oxygen species, caused cell death by apoptosis^{11,38}. Moreover, calpain activity, involved in Stx1-mediated caspase-8 cleavage and apoptosis, is calcium-dependent³⁹. The ribosome-inactivating RNA *N*-glycosidase activity of ricin was shown to be divalent cation-dependent⁴⁰. Taken together, the effects of Stx1 on inhibition of protein synthesis and the induction of apoptosis are calcium-dependent, thus NF449 could affect these intracellular pathways by inhibiting calcium influx, thereby exerting a protective effect.

In calcium-free medium Stx1B does not induce calcium influx¹⁴, indicating that the elevated calcium originates from an extracellular source. NF449 did not affect the transport of the toxin to the ER, while BAPTA-AM (the positive control) did (Fig. 3). BAPTA-AM is a cell permeable version of BAPTA that can chelate intracellular divalent cations with high specificity for Ca^{2+} , leaving minimal levels of free intracellular Ca^{2+} , whereas NF449

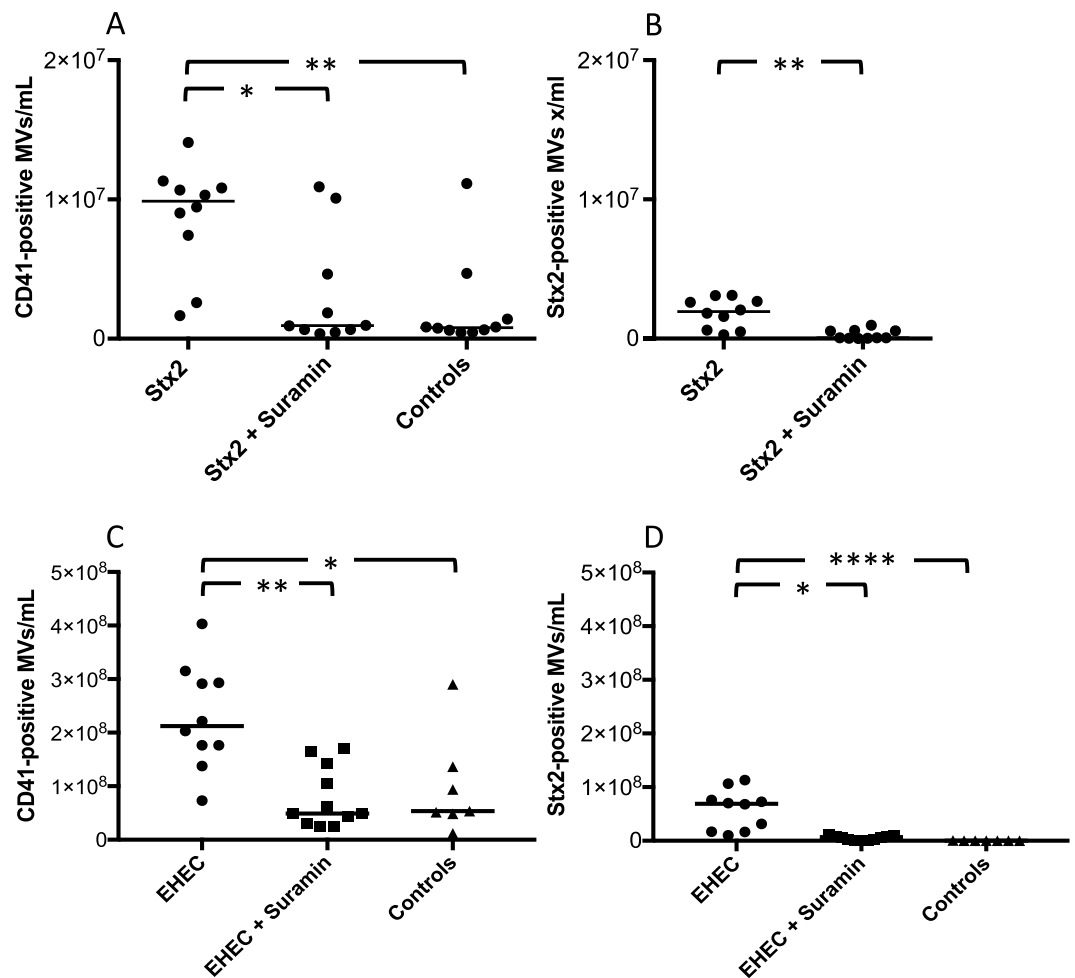


Figure 6. Suramin inhibits Shiga toxin 2- and EHEC-induced platelet-derived microvesicles and Shiga toxin 2-positive microvesicle-release *in vivo*. (**A** and **B**) Mice were pretreated with suramin or vehicle followed by injection of Shiga toxin 2 (Stx2) or PBS control (n = 10). (**A**) Stx2-injected mice had significantly higher levels of circulating platelet-derived microvesicles (MV, CD41+) and suramin pretreatment reduced this effect. (**B**) Stx2-positive microvesicles were significantly lower in mice pretreated with suramin. (**C** and **D**) Mice were inoculated with EHEC (n = 10) and certain mice were pretreated with suramin (n = 11) or inoculated with vehicle (n = 7). (**C**) EHEC-inoculated mice had significantly higher levels of circulating platelet-derived microvesicles compared to mice pretreated with suramin and PBS-treated mice. (**D**) Stx2-positive microvesicles were significantly higher in EHEC-inoculated mice and suramin pretreatment significantly lowered this effect. Median microvesicles/mL is denoted by the bar. *P < 0.05, **P < 0.01, ****P < 0.0001, two-tailed Mann-Whitney test (panel B) and Kruskal-Wallis test (panel A, C and D).

affects Ca^{2+} influx into cells, but not intracellular Ca^{2+} sources. As NF449 does not perturb intracellular Ca^{2+} sources this may explain why toxin transport to the ER was not affected.

The P2X receptors differ in the number of their subunits, from 1 to 7, and these subunits share a certain degree of homology⁴¹. NF449 is considered highly selective for the P2X1 receptor even at nanomolar concentrations^{32,42}. Concentrations in the micromolar range, such as used by others^{43,44} and in the current study, have a higher P2X1 antagonist potency, but even a certain effect on other purinergic receptors³². P2X1 receptor silencing followed by caspase detection after challenging HeLa cells with Stx1 showed a protective effect similar to NF449 blockade. The effect of ATP blockade on calcium influx *in vitro*, and microvesicle release *in vitro* and *in vivo*, was also confirmed using the non-selective P2X antagonist, suramin, with a varying effect on all P2X receptors³².

Stx2 induces the release of microvesicles from blood cells¹⁸ and, as shown here, Stx1 and Stx2 induce the release of microvesicles from HeLa cells and platelets. Microvesicles contain cytosolic content from their parent cell, and, in the case of a toxin-affected cell, the microvesicles will carry toxin and thereby transfer their cargo to a recipient cell¹⁶. This mechanism of transfer of injurious substances via microvesicles will evade the host response as the toxin will be protected by host membranes. Thus, a substance capable of decreasing microvesicle release could be protective, in conditions in which microvesicles promote disease in general^{45,46}, and in Stx-mediated disease in particular. NF449 inhibited Stx-induced microvesicle release from HeLa cells and platelets, and suramin reduced microvesicle release from platelets, both *in vitro* and *in vivo*. Calcium influx is required for microvesicle

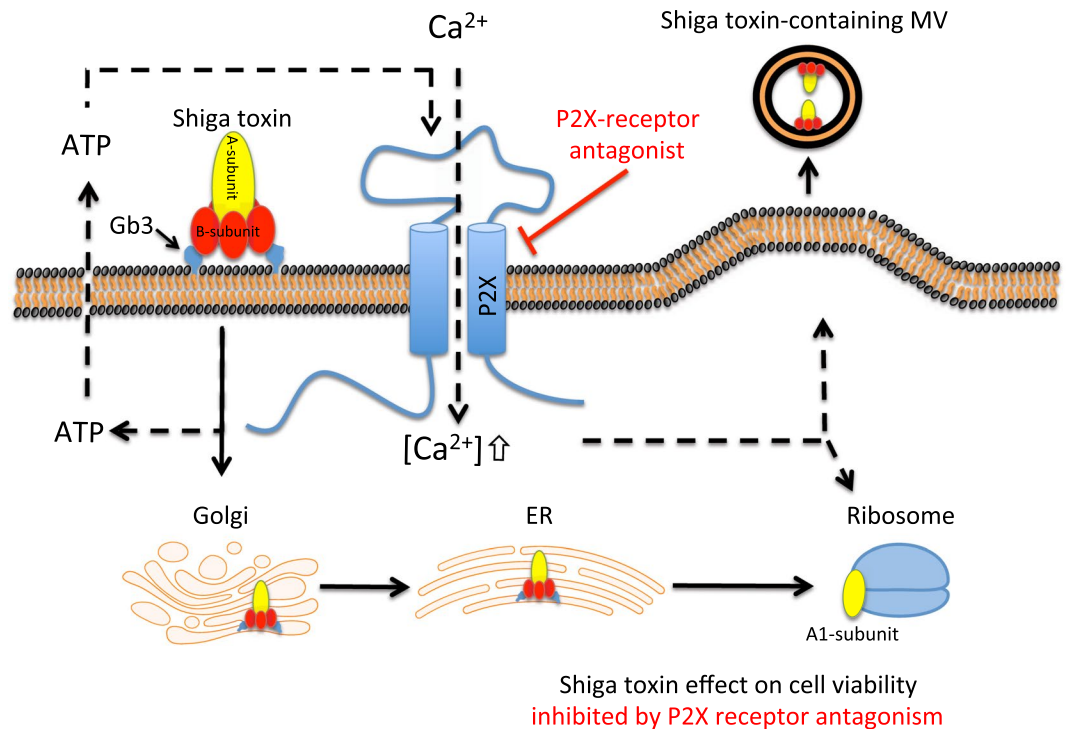


Figure 7. Proposed mechanism of Shiga toxin induced cellular activation via ATP. Schematic diagram displaying a proposed mechanism by which Shiga toxin induces cellular activation, utilizing ATP as a second messenger. When Shiga toxin binds to its receptor, globotriaosylceramide (Gb3), cells release ATP. ATP in turn binds to P2X receptors causing Ca^{2+} -influx into the cell. Ca^{2+} is necessary for intracellular processes associated with Shiga toxin induced cell death and the shedding of toxin-positive microvesicles (MVs). Purinergic receptor blockade, such as NF449 and suramin, used in this study, block P2X-activation and these Shiga toxin-mediated effects. Filled arrows show the transport route of Shiga toxin and dashed arrows show ATP-mediated signaling. ER: endoplasmic reticulum. This illustration was created using software from Motifolio.

shedding⁴⁷ and thus the decreased microvesicle release in the presence of NF449 and suramin would presumably be associated with blocked calcium influx via the P2X1 receptor⁴⁸.

Suramin is used commercially for the treatment of parasite infections in humans⁴⁹ as well as autistic spectrum disorders in mouse models⁵⁰. In a recent study we reported that red blood cells stimulated with Stx2 released microvesicles, an effect modulated by the non-selective P2X receptor inhibitors suramin and PPADS¹⁵. We propose that the beneficial effects of NF449 and suramin on microvesicle release should be further explored as microvesicles have been associated with the transfer of deleterious substances in various disease states⁴⁶.

We conclude that Stx induces an intracellular signal via ATP interaction with purinergic receptors allowing calcium influx and promoting the injurious effects of the toxin on cell viability, the inhibition of protein synthesis and apoptosis. Furthermore, the ATP-induced signal stimulates microvesicle release from cells. This may be a protective mechanism by which cells rid themselves of toxic substances but may also promote disease, as these microvesicles circulate with toxic content thus reaching the kidney which is the target organ¹⁶. We demonstrate that purinergic P2X blockade abrogated the injurious effects of Stx related to calcium influx, viability and microvesicle release and therefore suggest purinergic signaling as a novel mechanism of Stx-mediated cellular injury. Purinergic signaling blockade should be explored as a novel therapeutic option in Stx-mediated disease.

Methods

HeLa cells and platelets. HeLa cells were cultured in Dulbecco's Modified Eagle Medium (DMEM, Invitrogen, Paisley, UK) with supplements and seeded at a density of 10^5 cells/mL 24 hours before the start of experiments, as described in the supplement.

For the isolation of platelet-rich-plasma, blood was drawn from healthy adult donors into Vacutainer tubes (Becton Dickinson, Franklin Lanes, NJ) containing Lepirudin (50 $\mu\text{g}/\text{mL}$, Refludan, Celgene, Windsor, UK), as detailed in the supplement. The study was performed with the approval of the Regional Ethics Review Board of Lund University, the written informed consent of the subjects (healthy adult donors) in accordance with relevant guidelines and regulations.

Detection of the P2X1 receptor on HeLa cells and platelets. The presence of the P2X1 receptor on HeLa cells and platelets was confirmed by immunoblotting (see description in the supplement) using an anti-P2X1 primary antibody (1 $\mu\text{g}/\text{mL}$, ab74058, Abcam, Cambridge, UK). The observed band corresponded to approximately 60 kDa, which is the receptor size reported for P2X1³⁵, shown in Supplementary Fig. S6.

P2X1 silencing. P2X1 mRNA in HeLa cells was silenced by RNA interference. Immunoblotting was performed to confirm protein reduction (Supplementary Fig. S7), described in the supplement.

Shiga toxins. Stx1 and Stx2 were obtained from the Phoenix Lab (Phoenix Lab, Tufts Medical Center, Boston, MA). In certain experiments Alexa:488-conjugated Stx1B-subunit⁵¹ was used. For details see the supplement.

Detection of ATP. Detection of ATP in mouse plasma and medium from HeLa cells was carried out using firefly luciferase by a bioluminescence assay, as described in the supplement.

Phosphate determination assay. Free phosphate groups in media from HeLa cells stimulated with Stx1, PBS or calcium ionophore were detected using a Phosphate assay kit (Sigma-Aldrich, Saint Louis, MO), as detailed in the supplement.

NF449. NF449 (Tocris Bioscience, Bristol, UK) was used as a specific P2X1 receptor antagonist⁴² at a concentration of 60 μ M, unless otherwise stated. NF449 did not bind to Stx1 or Stx2 in the fluid phase, nor did it affect Stx binding to cells, its uptake or intracellular cleavage as further described in the supplement and Supplementary Fig. S8 (binding) and S9 (uptake).

Suramin. Suramin (Sigma-Aldrich) is a non-selective P2X receptor antagonist²⁶, which was used for *in vitro* and *in vivo* experiments described below.

Calcium influx assay. Calcium concentrations in HeLa cells and platelet-rich-plasma were measured using Fluo-4 NW (Thermo Fisher Scientific), as described in the supplementary methods.

Stx1B-subunit retrograde transport to the endoplasmic reticulum. Retrograde trafficking of Stx1B to the endoplasmic reticulum was detected by a previously described method⁵², using HeLa cells transfected with a SNAP-tag localized to the ER and benzylguanine-labeled Stx1B, as described in the supplement.

Viability assay. The viability of HeLa cells exposed to Stx was assessed using Alamar Blue (Thermo Fisher Scientific). The viability of PBS-treated cells was defined as 100%. Details are given in the supplement.

Protein synthesis assay. HeLa cell protein synthesis was assessed by [³⁵S]-methionine protein incorporation. Values are presented as counts per minute from [³⁵S] incorporated into newly synthesized protein divided by total protein concentration, as described in the supplement.

Caspase 3/7 apoptosis assay. Apoptosis assays were carried out using CellEvent Caspase-3/7 reagent and NucBlue nuclear staining (both from Thermo Fisher Scientific). Fluorescence emitted from HeLa cells was measured and divided by the number of cell nuclei, see the supplement.

Isolation and detection of microvesicles from HeLa cells and platelets. HeLa cells were stimulated with Stx1B:Alexa488 or Stx2. Microvesicles were isolated and labeled with mouse anti-CD44PE and rabbit anti-Stx2 (BEI resources, Manassas, VA) and swine anti-rabbit FITC (Dako, Glostrup, Denmark), both diluted in 0.1% saponin (Sigma-Aldrich). Platelets were stimulated with Stx1 or Stx2. Microvesicles were isolated and labeled with mouse anti-CD42PE and mouse anti-Stx1 (Santa Cruz Biotechnology, Dallas, TX) and goat anti-mouse FITC (Dako), both diluted in 0.1% saponin, or rabbit anti-Stx2 as above. The procedure is detailed in the supplement.

Mice. BALB/c wild-type mice were bred in the animal facilities of the Biomedical Service Division, Medical Faculty, Lund. Both female and male mice were used at 8–13 weeks of age and were age-matched. All animal experiments were approved by the animal ethics committee of Lund University and carried out in accordance with the guidelines of the Swedish National Board of Agriculture and the EU directive for the protection of animals used in science. Approval numbers M13–14 and M148–16.

Shiga toxin 2-injection mouse model. Stx2 was injected intraperitoneally at 285, 142.5 or 71.25 ng/kg body weight and control mice received PBS, as previously described²⁷. Mice were monitored daily. In the Stx2-injection model mice usually show symptoms on day 3. For microvesicle counts mice were sacrificed on day 3 and for ATP assay mice were sacrificed upon showing signs of disease or on day 7. The procedure is detailed in the supplement.

Escherichia coli O157:H7-infection mouse model. Mice were infected with *E. coli* O157:H7 (10^8 CFU/mouse) as previously described^{27,53}. Mice were sacrificed on day 3 after inoculation, before the development of symptoms. Blood was collected for microvesicle analysis as described above. See the supplement for details.

Treatment of Stx2-injected and EHEC-infected mice with suramin. BALB/c mice were injected intraperitoneally with suramin and control mice received vehicle 16 hours before injection of Stx2 intraperitoneally or one hour before inoculation with *E. coli* O157:H7 or its corresponding vehicle. All mice were sacrificed on day 3 post inoculation and samples were collected for microvesicle analysis, as described in the supplement.

Isolation and labeling of murine microvesicles. Microvesicles were isolated and labeled as previously described¹⁶. Platelet microvesicles were detected with rat anti-mouse CD41:APC (BD Biosciences) and Stx2-containing microvesicles were detected as described above. See the supplement for details.

Flow cytometry for detection of cells and microvesicles. Cells were analyzed using a FACSCanto™II flow cytometer (BD Immunocytometry Systems, San Jose, CA) and microvesicles were analyzed using a CyFlow Cube 8 (Sysmex Partec, Görlitz, Germany), as described in the supplement.

Statistical analysis. Differences between groups were assessed by the two-tailed Mann-Whitney U test, or by the Kruskal-Wallis multiple-comparison test when comparing more than two groups, followed by comparison between specific groups using the Dunn procedure. For calcium influx repeated measurements two-way repeated measures ANOVA was used. All statistical analyses were calculated using Prism 7 version 7.0a (GraphPad, La Jolla, CA).

Data Availability

Data are described in the supplement and available from the corresponding author upon request.

References

- O'Brien, A. D. & Holmes, R. K. Shiga and Shiga-like toxins. *Microbiol Rev* **51**, 206–220 (1987).
- Fraser, M. E., Cherniaia, M. M., Kozlov, Y. V. & James, M. N. Crystal structure of the holotoxin from Shigella dysenteriae at 2.5 Å resolution. *Nat Struct Biol* **1**, 59–64 (1994).
- Endo, Y. *et al.* Site of action of a Vero toxin (VT2) from *Escherichia coli* O157:H7 and of Shiga toxin on eukaryotic ribosomes. RNA N-glycosidase activity of the toxins. *Eur J Biochem* **171**, 45–50 (1988).
- Gallegos, K. M. *et al.* Shiga toxin binding to glycolipids and glycans. *PLoS One* **7**, e30368 (2012).
- Romer, W. *et al.* Shiga toxin induces tubular membrane invaginations for its uptake into cells. *Nature* **450**, 670–675 (2007).
- Garred, O., van Deurs, B. & Sandvig, K. Furin-induced cleavage and activation of Shiga toxin. *J Biol Chem* **270**, 10817–10821 (1995).
- Obrig, T. G., Moran, T. P. & Brown, J. E. The mode of action of Shiga toxin on peptide elongation of eukaryotic protein synthesis. *Biochem J* **244**, 287–294 (1987).
- Sandvig, K. & van Deurs, B. Endocytosis, intracellular transport, and cytotoxic action of Shiga toxin and ricin. *Physiol Rev* **76**, 949–966 (1996).
- Békássy, Z. D. *et al.* Intestinal damage in enterohemorrhagic *Escherichia coli* infection. *Pediatr Nephrol* **26**, 2059–2071 (2011).
- Karpman, D. *et al.* Apoptosis of renal cortical cells in the hemolytic-uremic syndrome: *in vivo* and *in vitro* studies. *Infect Immun* **66**, 636–644 (1998).
- Fujii, J. *et al.* Rapid apoptosis induced by Shiga toxin in HeLa cells. *Infect Immun* **71**, 2724–2735 (2003).
- Karpman, D. & Ståhl, A. L. Enterohemorrhagic *Escherichia coli* pathogenesis and the host response. *Microbiol Spectr* **2**, (2014).
- Lee, M. S. & Tesh, V. L. Roles of Shiga Toxins in Immunopathology. *Toxins (Basel)* **11**, (2019).
- Klokk, T. I., Kavaliauskiene, S. & Sandvig, K. Cross-linking of glycosphingolipids at the plasma membrane: consequences for intracellular signaling and traffic. *Cell Mol Life Sci* **73**, 1301–1316 (2016).
- Arvidsson, I. *et al.* Shiga toxin-induced complement-mediated hemolysis and release of complement-coated red blood cell-derived microvesicles in hemolytic uremic syndrome. *J Immunol* **194**, 2309–2318 (2015).
- Ståhl, A. L. *et al.* A novel mechanism of bacterial toxin transfer within host blood cell-derived microvesicles. *PLoS Pathog* **11**, e1004619 (2015).
- Ståhl, A. L., Sartz, L. & Karpman, D. Complement activation on platelet-leukocyte complexes and microparticles in enterohemorrhagic *Escherichia coli*-induced hemolytic uremic syndrome. *Blood* **117**, 5503–5513 (2011).
- Ståhl, A. L., Sartz, L., Nelsson, A., Békássy, Z. D. & Karpman, D. Shiga toxin and lipopolysaccharide induce platelet-leukocyte aggregates and tissue factor release, a thrombotic mechanism in hemolytic uremic syndrome. *PLoS One* **4**, e6990 (2009).
- Hugel, B., Martinez, M. C., Kunzelmann, C. & Freyssinet, J. M. Membrane microparticles: two sides of the coin. *Physiology (Bethesda)* **20**, 22–27 (2005).
- Morel, O., Jesel, L., Freyssinet, J. M. & Toti, F. Cellular mechanisms underlying the formation of circulating microparticles. *Arterioscler Thromb Vasc Biol* **31**, 15–26 (2011).
- Ståhl, A. L., Johansson, K., Mossberg, M., Kahn, R. & Karpman, D. Exosomes and microvesicles in normal physiology, pathophysiology, and renal diseases. *Pediatr Nephrol*, (2019).
- Menzies, R. I., Tam, F. W., Unwin, R. J. & Bailey, M. A. Purinergic signaling in kidney disease. *Kidney Int* **91**, 315–323 (2017).
- Harden, T. K., Boyer, J. L. & Nicholas, R. A. P2-purinergic receptors: subtype-associated signaling responses and structure. *Annu Rev Pharmacol Toxicol* **35**, 541–579 (1995).
- Mahaut-Smith, M. P., Taylor, K. A. & Evans, R. J. Calcium signalling through ligand-gated ion channels such as P2X1 receptors in the platelet and other non-excitabile cells. *Adv Exp Med Biol* **898**, 305–329 (2016).
- Hulsmann, M. *et al.* NF449, a novel picomolar potency antagonist at human P2X1 receptors. *Eur J Pharmacol* **470**, 1–7 (2003).
- Lambertucci, C. *et al.* Medicinal chemistry of P2X receptors: agonists and orthosteric antagonists. *Curr Med Chem* **22**, 915–928 (2015).
- Calderon Toledo, C. *et al.* Shiga toxin-mediated disease in MyD88-deficient mice infected with *Escherichia coli* O157:H7. *Am J Pathol* **173**, 1428–1439 (2008).
- Calderon Toledo, C., Arvidsson, I. & Karpman, D. Cross-reactive protection against enterohemorrhagic *Escherichia coli* infection by enteropathogenic *E. coli* in a mouse model. *Infect Immun* **79**, 2224–2233 (2011).
- Römer, W. *et al.* Actin dynamics drive membrane reorganization and scission in clathrin-independent endocytosis. *Cell* **140**, 540–553 (2010).
- Ghosh, S. A., Polanowska-Grabowska, R. K., Fujii, J., Obrig, T. & Gear, A. R. Shiga toxin binds to activated platelets. *J Thromb Haemost* **2**, 499–506 (2004).
- Pasquet, J. M., Dachary-Prigent, J. & Nurden, A. T. Calcium influx is a determining factor of calpain activation and microparticle formation in platelets. *Eur J Biochem* **239**, 647–654 (1996).
- Rettinger, J. *et al.* Profiling at recombinant homomeric and heteromeric rat P2X receptors identifies the suramin analogue NF449 as a highly potent P2X1 receptor antagonist. *Neuropharmacology* **48**, 461–468 (2005).
- Karpman, D., Loos, S., Tati, R. & Arvidsson, I. Haemolytic uraemic syndrome. *J Intern Med* **281**, 123–148 (2017).
- Fung, C. Y. *et al.* Platelet Ca(2+) responses coupled to glycoprotein VI and Toll-like receptors persist in the presence of endothelial-derived inhibitors: roles for secondary activation of P2X1 receptors and release from intracellular Ca(2+) stores. *Blood* **119**, 3613–3621 (2012).
- Clifford, E. E., Parker, K., Humphreys, B. D., Kertesz, S. B. & Dubyak, G. R. The P2X1 receptor, an adenosine triphosphate-gated cation channel, is expressed in human platelets but not in human blood leukocytes. *Blood* **91**, 3172–3181 (1998).
- McConkey, D. J. & Orrenius, S. Signal transduction pathways to apoptosis. *Trends Cell Biol* **4**, 370–375 (1994).
- Fabbrini, M. S., Katayama, M., Nakase, I. & Vago, R. Plant ribosome-inactivating proteins: progresses, challenges and biotechnological applications (and a few digressions). *Toxins (Basel)* **9**, (2017).
- Narayanan, S., Surolia, A. & Karande, A. A. Ribosome-inactivating protein and apoptosis: abrin causes cell death via mitochondrial pathway in Jurkat cells. *Biochem J* **377**, 233–240 (2004).

39. Lee, S. Y., Lee, M. S., Cherla, R. P. & Tesh, V. L. Shiga toxin 1 induces apoptosis through the endoplasmic reticulum stress response in human monocytic cells. *Cell Microbiol* **10**, 770–780 (2008).
40. Gluck, A. & Wool, I. G. Dependence of depurination of oligoribonucleotides by ricin A-chain on divalent cations and chelating agents. *Biochem Mol Biol Int* **39**, 285–291 (1996).
41. Shieh, C. C., Jarvis, M. F., Lee, C. H. & Perner, R. J. P2X receptor ligands and pain. *Expert Opin Ther Pat* **16**, 1113–1127 (2006).
42. Kassack, M. U. *et al.* Structure-activity relationships of analogues of NF449 confirm NF449 as the most potent and selective known P2X1 receptor antagonist. *Eur J Med Chem* **39**, 345–357 (2004).
43. Fagerberg, S. K., Jakobsen, M. R., Skals, M. & Praetorius, H. A. Inhibition of P2X receptors protects human monocytes against damage by Leukotoxin from *Aggregatibacter actinomycetemcomitans* and alpha-Hemolysin from *Escherichia coli*. *Infect Immun*. **84**, 3114–3130 (2016).
44. Casati, A. *et al.* Cell-autonomous regulation of hematopoietic stem cell cycling activity by ATP. *Cell Death Differ*. **18**, 396–404 (2011).
45. Ohno, S., Ishikawa, A. & Kuroda, M. Roles of exosomes and microvesicles in disease pathogenesis. *Adv Drug Deliv Rev*. **65**, 398–401 (2013).
46. Karpman, D., Ståhl, A. L. & Arvidsson, I. Extracellular vesicles in renal disease. *Nat Rev Nephrol* **13**, 545–562 (2017).
47. Boulanger, C. M., Amabile, N. & Tedgui, A. Circulating microparticles: a potential prognostic marker for atherosclerotic vascular disease. *Hypertension*. **48**, 180–186 (2006).
48. Varga-Szabo, D., Braun, A. & Nieswandt, B. Calcium signaling in platelets. *J Thromb Haemost*. **7**, 1057–1066 (2009).
49. Singh Grewal, A., Pandita, D., Bhardwaj, S. & Lather, V. Recent updates on development of drug molecules for human African Trypanosomiasis. *Curr Top Med Chem*. **16**, 2245–2265 (2016).
50. Naviaux, R. K. *et al.* Antipurinergic therapy corrects the autism-like features in the poly(IC) mouse model. *PLoS One*. **8**, e57380 (2013).
51. Renard, H. F. *et al.* Endophilin-A2 functions in membrane scission in clathrin-independent endocytosis. *Nature*. **517**, 493–496 (2015).
52. Geiger, R., Luisoni, S., Johnsson, K., Greber, U. F. & Helenius, A. Investigating endocytic pathways to the endoplasmic reticulum and to the cytosol using SNAP-trap. *Traffic* **14**, 36–46 (2013).
53. Chromek, M., Arvidsson, I. & Karpman, D. The antimicrobial peptide cathelicidin protects mice from *Escherichia coli* O157:H7-mediated disease. *PLoS One*. **7**, e46476 (2012).

Acknowledgements

This project was funded by the Swedish Research Council (K2013–64X-14008–13–5, K2015–99X-22877–01–6 and 2017–01920), The Knut and Alice Wallenberg Foundation (Wallenberg Clinical Scholar 2015.0320), The Torsten Söderberg Foundation, Skåne Centre of Excellence in Health, The IngaBritt and Arne Lundberg’s Research Foundation, Olle Engkvist Byggmästare Foundation, Crown Princess Lovisa’s Society for Child Care, Region Skåne and The Konung Gustaf V:s 80-årsfond (all to DK). Sebastian Loos was supported by a research fellowship from the Deutsche Forschungsgemeinschaft (LO 2021/2–1).

Author Contributions

K.E.J., A-L.S., I.A., S.L., A.T., J.R., M.C. and A-C.K., designed and conducted experiments. L.J. designed experiments and contributed materials. K.E.J., A-L. S., I.A., S.L., A.T., J.R., M.C., A-C.K. and D.K. analyzed data. K.E.J. and D.K. wrote the manuscript. All authors read and approved the final manuscript.

Additional Information

Supplementary information accompanies this paper at <https://doi.org/10.1038/s41598-019-50692-1>.

Competing Interests: The authors declare no competing interests.

Publisher’s note Springer Nature remains neutral with regard to jurisdictional claims in published maps and institutional affiliations.



Open Access This article is licensed under a Creative Commons Attribution 4.0 International License, which permits use, sharing, adaptation, distribution and reproduction in any medium or format, as long as you give appropriate credit to the original author(s) and the source, provide a link to the Creative Commons license, and indicate if changes were made. The images or other third party material in this article are included in the article’s Creative Commons license, unless indicated otherwise in a credit line to the material. If material is not included in the article’s Creative Commons license and your intended use is not permitted by statutory regulation or exceeds the permitted use, you will need to obtain permission directly from the copyright holder. To view a copy of this license, visit <http://creativecommons.org/licenses/by/4.0/>.

© The Author(s) 2019

Shiga toxin signals via ATP and its effect is blocked by purinergic receptor antagonism

Karl E. Johansson, Anne-Lie Ståhl, Ida Arvidsson, Sebastian Loos, Ashmita Tontanahal, Johan Rebetz, Milan Chromek, Ann-Charlotte Kristoffersson, Ludger Johannes, Diana Karpman

Supplementary information

Complete methods

HeLa cells and platelets

HeLa cells were cultured in Dulbecco's Modified Eagle Medium (DMEM, Invitrogen, Paisley, UK) supplemented with 10% fetal bovine serum and 1% penicillin-streptomycin. Cells were cultured in a cell incubator with 5 % CO₂ in 37°C. HeLa cells were seeded at a density of 10⁵ cells/mL 24 hours before the start of experiments.

For the isolation of platelet-rich-plasma, blood was drawn from healthy adult donors into Vacutainer tubes (Becton Dickinson, Franklin Lanes, NJ) containing Lepirudin (50 µg/mL, Refludan, Celgene, Windsor, UK) via venipuncture, using a butterfly needle (Terumo Medical products, Hangzhou, China). The first blood tube (2.7 ml) was discarded. Whole blood was centrifuged at 170 x g for 15 min and the supernatant, containing platelet-rich-plasma, was collected. The study was performed with the approval of the Regional Ethics Review Board of Lund University and the written informed consent of the subjects (healthy adult donors) and in accordance with the relevant guidelines and regulations.

Detection of the P2X1 receptor on HeLa cells and platelets

The presence of the P2X1 receptor on HeLa cells and platelets was confirmed by immunoblotting. Cells were lysed in RIPA lysis buffer (0.15 M NaCl, 30 mM HEPES, 1% Triton X-100, 1% sodium deoxycholate and 0.1% sodium dodecyl sulfate). Whole cell lysate proteins were reduced with 2-mercaptoethanol (Sigma-Aldrich, Saint Louis, MO), separated by SDS-PAGE and transferred to a nitrocellulose membrane. The P2X1 receptor was stained with anti-P2X1 primary antibody (1 µg/mL, ab74058, Abcam, Cambridge, UK) followed by anti-rabbit HRP as the secondary antibody (0.5 µg/mL, ab7171, Abcam). P2X1 is shown in Supplementary Figure S6. The size corresponds to approximately 60 kDa, as previously described.¹

P2X1 silencing

P2X1 mRNA in HeLa cells was silenced by RNA interference. Cells were transfected with a pool of three different siRNAs targeting P2X1 mRNA (siP2X1, 3 and 6 µM) or with a non-targeting control siRNA (siCtrl, 6 µM) using siRNA Transfection Reagent according to the manufacturer's instructions (Santa Cruz Biotechnology, Santa Cruz, CA). Experiments were carried out 48 h post-transfection. Immunoblotting was performed to confirm protein reduction (Supplementary Figure S7). Equal loading was determined by the stain-free method (BioRad, Hercules, CA). These cells were used for Caspase 3/7-detection, as described below.

Shiga toxins

Stx1 and Stx2 were obtained from the Phoenix Lab (Phoenix Lab, Tufts Medical Center, Boston, MA). LPS contamination was measured using the Limulus Amebocyte Lysate

method (Thermo Fisher Scientific, Rockford, IL) detecting small amounts (in Stx1 2.3 ng/mg toxin, in Stx2 183 ng/mg toxin). In certain experiments Alexa488-conjugated Stx1B-subunit² was used.

Detection of ATP

Detection of ATP was carried out using a bioluminescence assay. Mouse plasma was diluted 1:1000 in PBS and ATP content was analyzed using firefly luciferase to cleave phosphate groups (65 nM, Sigma-Aldrich) and D-luciferin (1.3 mM, Thermo Fisher Scientific) with detection at one-sec integration time in a Glomax Discover System (Promega, Fitchburg, WI). HeLa cells were incubated with Hank's Balanced Salt Solution with Ca²⁺/Mg²⁺ (HBSS, GE Life Sciences, Chicago, IL) supplemented with 20 mM HEPES for 5 min at 37°C followed by addition of Stx1 (1 µg/mL or 200 ng/mL) or Stx2 (1µg/mL). PBS (GE Life Sciences) was the negative control and histamine (100 µM, Sigma-Aldrich) was the positive control. After 5 min the cell medium was collected and added to 20x reaction buffer. The ATP concentration in the medium was measured using ATP determination kit (Thermo Fischer Scientific) according to the manufacturer's instructions.

Phosphate determination assay

HeLa cells were incubated with TRIS-buffered saline (Medicago, Uppsala, Sweden) supplemented with 1 mM CaCl₂, 0.4 mM MgSO₄ and 20 mM HEPES for 5 min at 37°C before addition of Stx1 (1 µg/mL), A23187 calcium ionophore as the positive control (10 µM, Sigma-Aldrich) or PBS. Supernatant was collected after 40 min and phosphate reagent (Phosphate assay kit, Abcam) was added to each sample and to the control (blank) samples, containing PBS that had not been in contact with the cells, according to

the manufacturer's instructions. After 30 min incubation at room temperature the absorbance of the samples was measured at 600 nm and the blank value was subtracted from each sample.

NF449

NF449 (Tocris Bioscience, Bristol, UK) is a specific P2X1 receptor antagonist.³ NF449 was used at a concentration of 60 μ M, unless otherwise stated.

In order to rule out a direct interaction between NF449 and Stx microtiter wells were coated with NF449 (120 μ M) in 0.1 M NaHCO₃ pH 9.3 (Merck, Darmstadt, Germany) at 4°C overnight. Wells were washed with PBS-Tween 0.05% (PBS-T, Medicago, Uppsala, Sweden) and blocked with bovine serum albumin (1%, BSA, Sigma-Aldrich) for 1 h. Wells were washed and incubated with Stx1 or Stx2 (1 μ g/mL in 1% BSA) for 1 h. After washing, wells were incubated with rabbit anti-Stx1 antibody (1:1000, List Labs, Campbell, CA) or rabbit anti-Stx2 (1:1000, BEI resources, Manassas, VA) for 1 h, washed and further incubated with anti-rabbit HRP antibody (1:1000, Dako, Glostrup, Denmark) for 1 hour. Microtiter wells were developed with SuperSignal ELISA Pico Chemiluminescent Substrate and luminescence was detected in a GloMax Discover System. No Stx binding could be detected, suggesting that there was no direct interaction between NF449 and Stx under these conditions.

Experiments were further carried out to determine if NF449 affected Stx1 binding to cells. HeLa cells were incubated with NF449 in PBS, or PBS alone, at 37°C for 1 h followed by incubation with Stx1B-subunit:Alexa 488 (1 μ g/mL), for 15 min, on ice to prevent toxin uptake. Cells were washed and detached with ice-cold EDTA (Versene,

Thermo Fisher Scientific) and analyzed by flow cytometry (described below). No difference in fluorescence could be detected by flow cytometry, indicating that NF449 did not affect Stx1B-binding (Supplementary Figure S8).

Experiments were designed to examine an effect of NF449 on toxin cellular uptake. HeLa cells were treated with NF449 or PBS for 30 min followed by incubation with Stx1 (1000, 200, 7 or 0 ng/mL) for 4 h at 37°C. Cells were washed with PBS and lysed in RIPA buffer. Cell lysate was transferred to white Maxisorp 96-well plates that were coated with mouse anti-Stx1 antibodies (2 µg/mL, STX1-3C10, Toxin Technology, Sarasota, FL) and blocked with 1 % BSA. The cell lysate was incubated for 1 h followed by detection with rabbit anti-Stx1 (1 µg/mL, List Biological Laboratories, Campbell, CA), goat anti-rabbit HRP (1:1000) and SuperSignal ELISA Pico Chemiluminescent Substrate (Thermo Fisher Scientific). Luminescence was detected in a GloMax Discover System. No difference between untreated and NF449-treated samples could be detected with regard to Stx1 uptake (Supplementary Figure S9).

Stx1 A-subunit has a molecular weight of 32 kDa and its intracellular cleavage product, A₁, is expected to have a molecular weight of 27.5 kDa.⁴ To investigate whether NF449 had an effect on cleavage of the Stx1 A-subunit, Stx1 was labeled with Iodine-125 (¹²⁵I) using Chloramine T (1 mg/mL) as an oxidant. HeLa cells were incubated with NF449 or with PBS for 30 minutes before addition of Stx1 (7 ng/mL) together with a trace amount of Stx1-¹²⁵I for 4 hours. The cells were lysed in RIPA buffer before separation by SDS-PAGE and transferred to a nitrocellulose membrane. The membrane was placed in an intensifying screen (Dupont Cronex Lightning Plus LE) with an X-ray film (Amersham Hyperfilm ECL, GE Healthcare) for three days at -80°C before development. In the

presence or absence of NF449 there was no difference in the ratio between uncleaved and cleaved Stx1A.

Suramin

Suramin (Sigma-Aldrich) is a non-selective P2X receptor antagonist,⁵ which was used for *in vitro* and *in vivo* experiments, described below.

Calcium influx assay

HeLa cells were incubated with Fluo-4 NW (Thermo Fisher Scientific) according to the manufacturer's instructions for 30 min at room temperature. In certain experiments NF449 or suramin (200 μ M), was added directly into the Fluo-4 NW solution at the same time point. HeLa cells were placed in an Axio Observer.A1 microscope (Zeiss, Oberkochen, Germany) at 37°C and the cells were allowed to settle for 15 min before the start of the experiment. Each well was monitored for a total of 300 sec and images were taken at 30-sec intervals. Stx1 (1 μ g/mL, this concentration was previously shown to induce calcium influx⁶), HBSS, as the negative control, or ATP (3 μ M), as the positive control, were added to the wells 30 sec after the start of the experiment and A23187 (10 μ M), was added after an additional 270 sec to induce fulminant calcium influx. Background signal was subtracted from the mean fluorescence intensity change of all cells in the field of view using ImageJ software (Version 1.48v, NIH, Bethesda).

Human platelet-rich-plasma was incubated with Fluo-4 NW, as above, and placed in a black 96-well plate with clear bottoms (Corning Inc., Corning, NY) in a GloMax Discover System at 37°C and further simultaneously stimulated with Stx1 or Stx2 (1 μ g/mL) and LPS from *E. coli* O157 (1 μ g/mL, a gift from R. Johnson, Public Health

Agency, Guelph, ON, Canada), with LPS alone or with PBS. LPS was added in order to activate the platelets and enable Stx binding, as previously shown.^{7,8} In experiments in which Stx2 was used apyrase (0.32 U/mL, Sigma-Aldrich) was added to enzymatically remove previously present ATP and reduce desensitization.⁹ Certain wells were pre-incubated with NF449. Initial fluorescence values (at 475 nm and 525/25 nm excitation and emission filters) were subtracted from 2 min post-stimulation values.

Stx1B-subunit retrograde transport to the endoplasmic reticulum

Retrograde trafficking of Stx1B to the ER was detected using a previously described method¹⁰ in which the cell is transfected with a SNAP-tag targeting the ER that covalently binds to benzylguanine conjugated to Stx1. The SNAP-tag transfected HeLa cells were treated with NF449, PBS or the intracellular calcium chelator BAPTA-AM as a control (10 μ M, Thermo Fisher Scientific) for 30 min, followed by incubation with Stx1B-subunit (1 μ g/mL) tagged with O⁶-benzylguanine (New England BioLabs, Ipswich, MA) on ice for an additional 30 min. The cells were washed three times with complete DMEM and incubated for 2 h at 37°C. SNAP-Cell Block (10 μ M, New England BioLabs) was added for 30 min. Cells were washed 3 times with PBS and lysed in RIPA-buffer on ice for 30 min. The lysate was added to a 96-well ELISA plate (Nunc, Roskilde, Denmark) that had been pre-coated with anti-SNAP antibody (A00684-40, GenScript, Biotech, Piscataway, NJ) diluted 1:2500 in NaCHO₃ (50mM, pH 9.6), blocked with 0.2 % bovine serum albumin (Sigma-Aldrich) followed by anti-Stx1 antibody (2 μ g/mL, STX1-3C10), secondary antibody anti-mouse biotinylated IgG (1:15000, Abcam) and streptavidin-peroxidase (1:5000, Sigma-Aldrich). Wells were developed with TMB Blue Substrate Chromogen (Agilent Technologies, Santa Clara, CA), acidified with sulfuric acid and absorbance was measured at 450 nm.

Viability assay

HeLa cells were incubated with Stx1 or Stx2 (7 ng/mL) or PBS control for 24 h in serum-free DMEM. Certain wells were pretreated with NF449 1 h before the toxin was added. Cell viability was assessed with Alamar Blue (Thermo Fisher Scientific) according to the manufacturer's instructions and analyzed using a GloMax Discover System. PBS-treated cells were defined as 100% viability.

Protein synthesis assay

HeLa cells were treated with NF449 or PBS for 30 min, followed by incubation with Stx1 (7 ng/mL) for 4 h. The cells were washed three times with PBS and incubated with [³⁵S]-labeled methionine diluted in methionine-free RPMI 1640 medium for 2 h. Cells were washed and lysed in RIPA-buffer. Full protein content of the lysates was precipitated in 14 % trichloroacetic acid followed by a wash in ice-cold acetone. Samples were diluted in scintillation liquid (Beckman Coulter, Brea, CA) and β-radiation was counted in a scintillation counter (LS 6500 Multi-Purpose Scintillation Counter, Beckman Coulter). Values are presented as counts per minute from [³⁵S] incorporated into newly synthesized protein divided by total protein concentration.

Caspase 3/7 apoptosis assay

HeLa cells were co-incubated with Stx1 (7 ng/mL) or the PBS vehicle and CellEvent Caspase-3/7 reagent (5 μM, Thermo Fisher Scientific). Certain wells were pre-treated with NF449 1 h before the toxin was added. After 24 h the cells were washed and incubated with HBSS containing 1 μg/mL NucBlue nuclear stain (Thermo Fisher Scientific) for 15 min. Cells were imaged in an Axio Observer.A1 microscope and the

fluorescence emitted with a 460 – 490 nm filter was measured and divided by the number of cell nuclei using ImageJ.

Isolation and detection of microvesicles from HeLa cells and platelets

HeLa cells were incubated in DMEM (Gibco, Carlsbad, CA) complemented with 0.1 % exosome-free fetal calf serum (Gibco) with or without NF449 for 1 h. Stx1B:Alexa488 (130 ng/mL) or Stx2 (200 ng/mL, both corresponding to 3 nM, a concentration that has previously been shown to cause microvesicle release from blood cells¹¹) in PBS, or PBS alone, was added to the cells and incubated for 40 min. Microvesicle-containing supernatant was collected and centrifuged at 300g for 10 min followed by centrifugation at 10000g for 15 min to remove cells and cellular debris.

For isolation of platelet microvesicles whole blood was diluted 1:1 with DMEM, incubated with NF449 or suramin (200 μ M) and stimulated with Stx1 or Stx2 (both at 200 ng/mL) or with PBS. Blood cells were removed by centrifugation at 2600g for 10 min and small platelets and cellular debris was removed by centrifugation at 10000g for 15 min. Microvesicles were fixed in 1% paraformaldehyde (PFA, HistoLab, Gothenburg, Sweden) for 30 min.

HeLa cell microvesicles were labeled with mouse anti-human CD44PE (1:400, eBioscience, Thermo Fisher Scientific) and platelets microvesicles were labeled with mouse anti-human CD42PE (1:80, Dako). For detection of Stx1 mouse anti-Stx1 (1.25 μ g/mL, Santa Cruz Biotechnology, Dallas, TX) and goat anti-mouse FITC (1:1000, Dako), both diluted in 0.1% saponin (Sigma-Aldrich), were used. Stx2 was detected using rabbit anti-Stx2 (1:200) and swine anti-rabbit FITC (1:2000, Dako), both diluted in

0.1% saponin. All antibody incubation times were 30 min. Microvesicles were washed with PBS and centrifuged at 20000g for 40 min and the pellet was saved. Buffers, cell medium and PFA were filtered through a 0.2 µm pore-size filter (Pall Corporation, Ann Arbor, MI) to reduce aggregates.

Mice

BALB/c wild-type mice were bred in the animal facilities of the Biomedical Service Division, Medical Faculty, Lund. Both female and male mice were used at 8–13 weeks of age and were age-matched. All animal experiments were approved by the animal ethics committee of Lund University in accordance to the guidelines of the Swedish National Board of Agriculture and the EU directive for the protection of animals used in science. Approval number M13-14 and M148-16.

Shiga toxin 2-injection mouse model

Purified Stx2 was diluted in PBS and injected intraperitoneally at a dose of 285, 142.5 or 71.25 ng/kg body weight for ATP assay and 285 ng/kg for microvesicle analysis and control mice received PBS vehicle at the same volume, as previously described.¹² Mice were monitored two to four times a day. Weight was taken daily and mice were observed for signs of disease (ruffled fur, lethargy, hunched posture, decreased activity, paralysis, tremor, ataxia and weight loss $\geq 20\%$), as previously described.¹² In the Stx2-injection model mice usually show symptoms from day 3 onwards. For microvesicle counts mice were sacrificed on day 3 and for ATP assay mice were sacrificed upon showing signs of symptoms or on day 7 (the defined end of the experiment). After isoflurane anesthesia blood was collected by heart puncture into citrated syringes, and the animals were sacrificed by cervical dislocation. For analysis of microvesicles blood was treated with

sterile-filtered PFA 4% (Histolab) at a final concentration of 2%.

***E. coli* O157:H7**

The Stx2-producing *E. coli* O157:H7 strain 86–24 (kindly provided by A. D. O'Brien, Uniformed Services University of the Health Sciences, Bethesda, MD) was previously characterized.¹³ Bacteria were grown, centrifuged and resuspended to a concentration of 10^9 colony forming units (CFU)/mL, as previously described.¹² Each mouse was inoculated with 10^8 CFU in a volume of 100 μ l.

***Escherichia coli* O157:H7-infection mouse model**

Mice were infected with *E. coli* O157:H7 according to a previously described infection protocol.¹² Mice were monitored two to four times a day. Weight was taken daily and mice were observed for signs of disease as previously described.¹² In this mouse model mice usually develop symptoms on day 6 and onwards. Mice were sacrificed on day 3 after inoculation, before the development of symptoms, to obtain microvesicle levels at this specific time-point. Before sacrifice mice were anesthetized with isoflurane, blood was collected for microvesicle analysis as described above. All mice were tested for bacteremia using blood culture flasks (Biomérieux inc, Durham, NC) and found to be negative.

Treatment of Stx2-injected and EHEC-infected mice with Suramin

BALB/c mice were injected intraperitoneally with suramin diluted in NaCl 0.9% at a dose of 60 mg/kg bodyweight and control mice received NaCl 0.9 % (vehicle) at the same volume 16 hours before injection of Stx2 intraperitoneally or with a suramin dose of 20 mg/kg body weight, or corresponding vehicle, one hour before inoculation with *E.*

coli O157:H7. All mice were sacrificed on day 3 post inoculation and samples were collected for microvesicle analysis.

Isolation and labeling of murine microvesicles

Microvesicles were isolated and labeled as previously described.¹¹ Briefly, whole blood from mice fixed in PFA was centrifuged to isolate microvesicles and to obtain a microvesicle-enriched suspension. Microvesicles from platelets were detected with rat anti-mouse CD41:APC (1:40, platelet marker) or IgG1:APC as an isotype control (both antibodies from BD Biosciences) and Stx-containing microvesicles were detected with polyclonal rabbit anti-Stx2 (1:200) and swine anti-rabbit:FITC (1:300, Dako, Glostrup, Denmark), both diluted in 0.1% saponin (Sigma-Aldrich).

Flow cytometry for detection of cells and microvesicles

FACSCantoTMII flow cytometer with a 488 nm laser and FACSDiva V.6.0 (BD Immunocytometry Systems, San Jose, CA) was used for flow cytometry measurements of cells. Forward scatter (FSC) and side scatter (SSC) channels were recorded with linear gain. The fluorescence channel was recorded at logarithmic gain and the flow rate was set to medium. Ten thousand events were counted in the population gate for each sample. Results are presented as percentage of Stx1B:Alexa488-positive cells and units of mean fluorescent intensity.

Flow cytometry for detection of microvesicles was performed using a CyFlow Cube 8 flow cytometer equipped with a 488 nm and a 638 nm laser (Sysmex Partec, Görlitz, Germany) and True Absolute Volumetric Counting (TVAC). Intuitive CyFlowTM acquisition and analysis software packages (Sysmex Partec) were used. The acquired data

files were analyzed using FCS Express 4 Flow Research Edition software (Version 4.07.0003, De Novo Software, Glendale, CA). Sheath fluid was pre-filtered (0.2 μm filter) and de-gassed before use. FSC and SSC and fluorescence channels were recorded in logarithmic mode. The microvesicle gate was set using Megamix beads (BioCytex, Marseille, France) to determine upper limits in both FSC (200) and SSC (240) signals and the lower limits were placed above the background level of the instrument and/or buffer which was determined by running 0.2 μm -filtered PBS. The detection threshold was set at a determined FSC. The spectral overlap of the fluorochromes used in this assay was compensated for using single-stained controls for each fluorochrome. A microvesicle was defined as an event positive for a specific cell marker and $<1 \mu\text{m}$ in size. Due to the detection limit of the flow cytometer particles below 100 nm in size are not detected. Results are presented as positive microvesicles after subtraction of the control antibody. A volume of 15 μl was counted for each sample on low flow rate (0.2 $\mu\text{l/s}$).

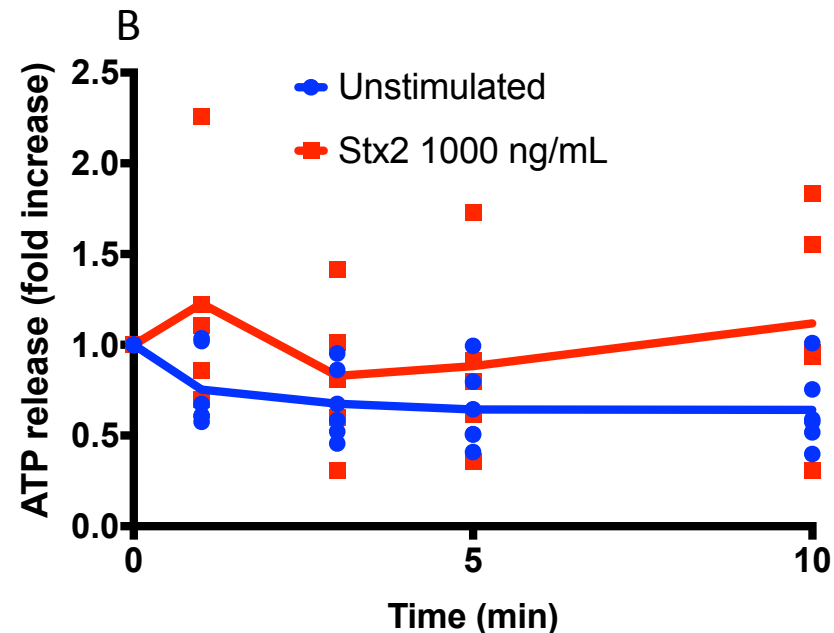
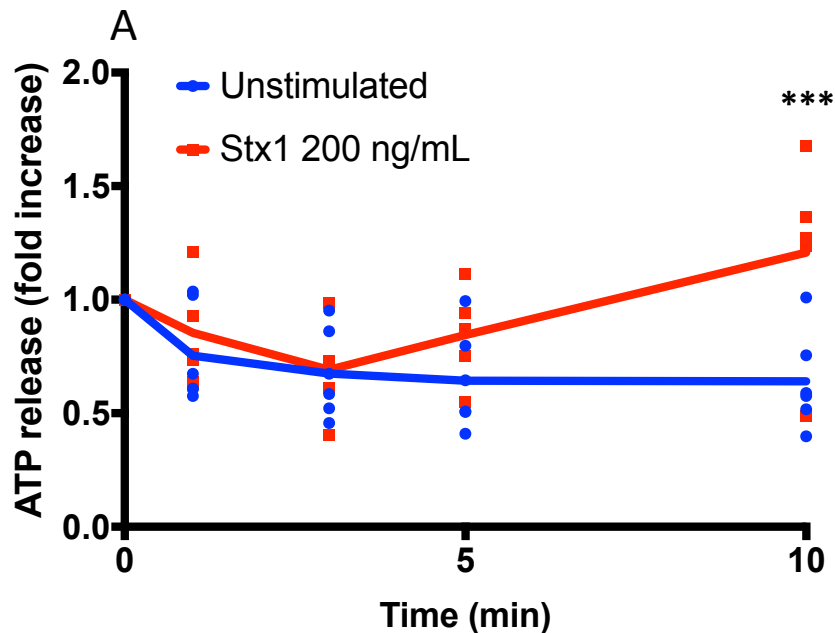
Statistical analysis

Differences between groups were assessed by the two-tailed Mann-Whitney U test, or by the Kruskal-Wallis multiple-comparison test when comparing more than two groups, followed by comparison between specific groups using the Dunn procedure. For calcium influx repeated measurements two-way repeated measures ANOVA was used. All statistical analyses were calculated using Prism 7 version 7.0a (GraphPad, La Jolla, CA).

References

- 1 Clifford, E. E., Parker, K., Humphreys, B. D., Kertesy, S. B. & Dubyak, G. R. The P2X1 receptor, an adenosine triphosphate-gated cation channel, is expressed in human platelets but not in human blood leukocytes. *Blood* **91**, 3172-3181, (1998).

- 2 Renard, H. F. *et al.* Endophilin-A2 functions in membrane scission in clathrin-independent endocytosis. *Nature*. **517**, 493-496, (2015).
- 3 Kassack, M. U. *et al.* Structure-activity relationships of analogues of NF449 confirm NF449 as the most potent and selective known P2X1 receptor antagonist. *Eur J Med Chem* **39**, 345-357, (2004).
- 4 Garred, O., van Deurs, B. & Sandvig, K. Furin-induced cleavage and activation of Shiga toxin. *J Biol Chem* **270**, 10817-10821, (1995).
- 5 Lambertucci, C. *et al.* Medicinal chemistry of P2X receptors: agonists and orthosteric antagonists. *Curr Med Chem* **22**, 915-928, (2015).
- 6 Klock, T. I., Kavaliauskiene, S. & Sandvig, K. Cross-linking of glycosphingolipids at the plasma membrane: consequences for intracellular signaling and traffic. *Cell Mol Life Sci*. **73**, 1301-1316, (2016).
- 7 Ståhl, A. L., Sartz, L., Nelsson, A., Békássy, Z. D. & Karpman, D. Shiga toxin and lipopolysaccharide induce platelet-leukocyte aggregates and tissue factor release, a thrombotic mechanism in hemolytic uremic syndrome. *PLoS One*. **4**, e6990, (2009).
- 8 Ghosh, S. A., Polanowska-Grabowska, R. K., Fujii, J., Obrig, T. & Gear, A. R. Shiga toxin binds to activated platelets. *J Thromb Haemost* **2**, 499-506, (2004).
- 9 Rolf, M. G., Brearley, C. A. & Mahaut-Smith, M. P. Platelet shape change evoked by selective activation of P2X1 purinoceptors with alpha,beta-methylene ATP. *Thromb Haemost* **85**, 303-308, (2001).
- 10 Geiger, R., Luisoni, S., Johnsson, K., Greber, U. F. & Helenius, A. Investigating endocytic pathways to the endoplasmic reticulum and to the cytosol using SNAP-trap. *Traffic* **14**, 36-46, (2013).
- 11 Ståhl, A. L. *et al.* A novel mechanism of bacterial toxin transfer within host blood cell-derived microvesicles. *PLoS Pathog*. **11**, e1004619, (2015).
- 12 Calderon Toledo, C. *et al.* Shiga toxin-mediated disease in MyD88-deficient mice infected with Escherichia coli O157:H7. *Am J Pathol* **173**, 1428-1439, (2008).
- 13 Bekassy, Z. D. *et al.* Intestinal damage in enterohemorrhagic Escherichia coli infection. *Pediatr Nephrol* **26**, 2059-2071, (2011).



Supplementary Figure S1: Shiga toxin induces release of ATP *in vitro*

HeLa cells were stimulated with PBS (n=6), Shiga toxin 1 (Stx1, 200 ng/mL, n=5) (A) or Shiga toxin 2 (Stx2, 1000 ng/mL, n=5) (B) and the ATP content was measured after 1, 3, 5 and 10 min. Data is presented as fold difference of initial ATP value. The median extracellular ATP content is depicted as the colored curve. ***: $P < 0.001$, two-way repeated measures ANOVA.

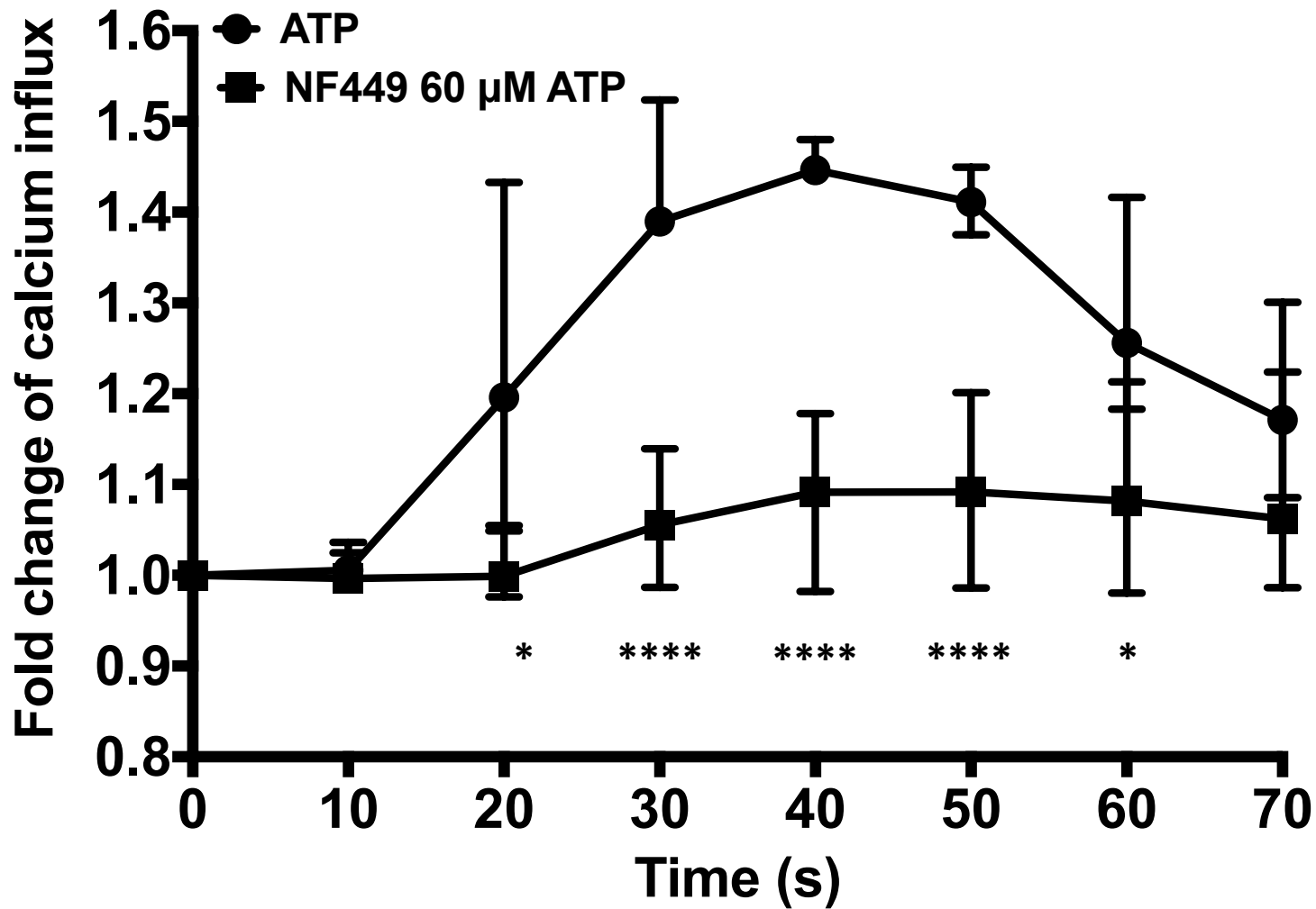


Figure S2: The effect of NF449 on calcium influx induced by ATP in HeLa cells

Calcium influx was measured in HeLa cells preincubated with NF449 (n=4) or PBS vehicle (n=3), stimulated with ATP (3 μM) and imaged by fluorescence microscopy. Results are shown as mean fluorescent change of all cells in the field of view and presented as median and range. *: P<0.05, ****: P<0.0001, two-way repeated measures ANOVA.

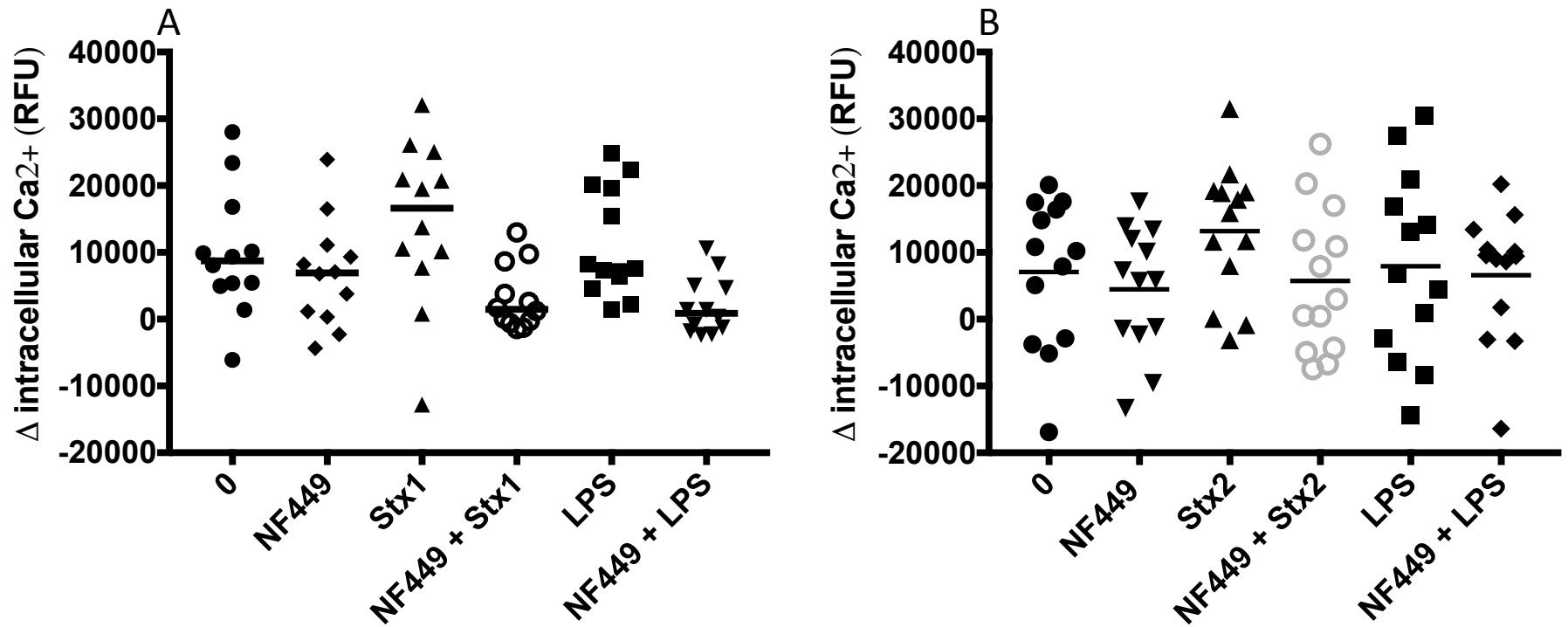


Figure S3: The effect of NF449 on calcium influx induced by Shiga toxin in platelets

Platelets (n=3 donors) were preincubated with NF449 or PBS vehicle followed by O157LPS, Stx1 (A) or Stx2 (B) or PBS vehicle. Data points for PBS-treated and NF449-treated platelets are the same as in Figure 2B and 2C. Data is presented as the initial fluorescence subtracted from fluorescence after 2 minutes. The median is denoted by the bar. RFU: relative fluorescent units.

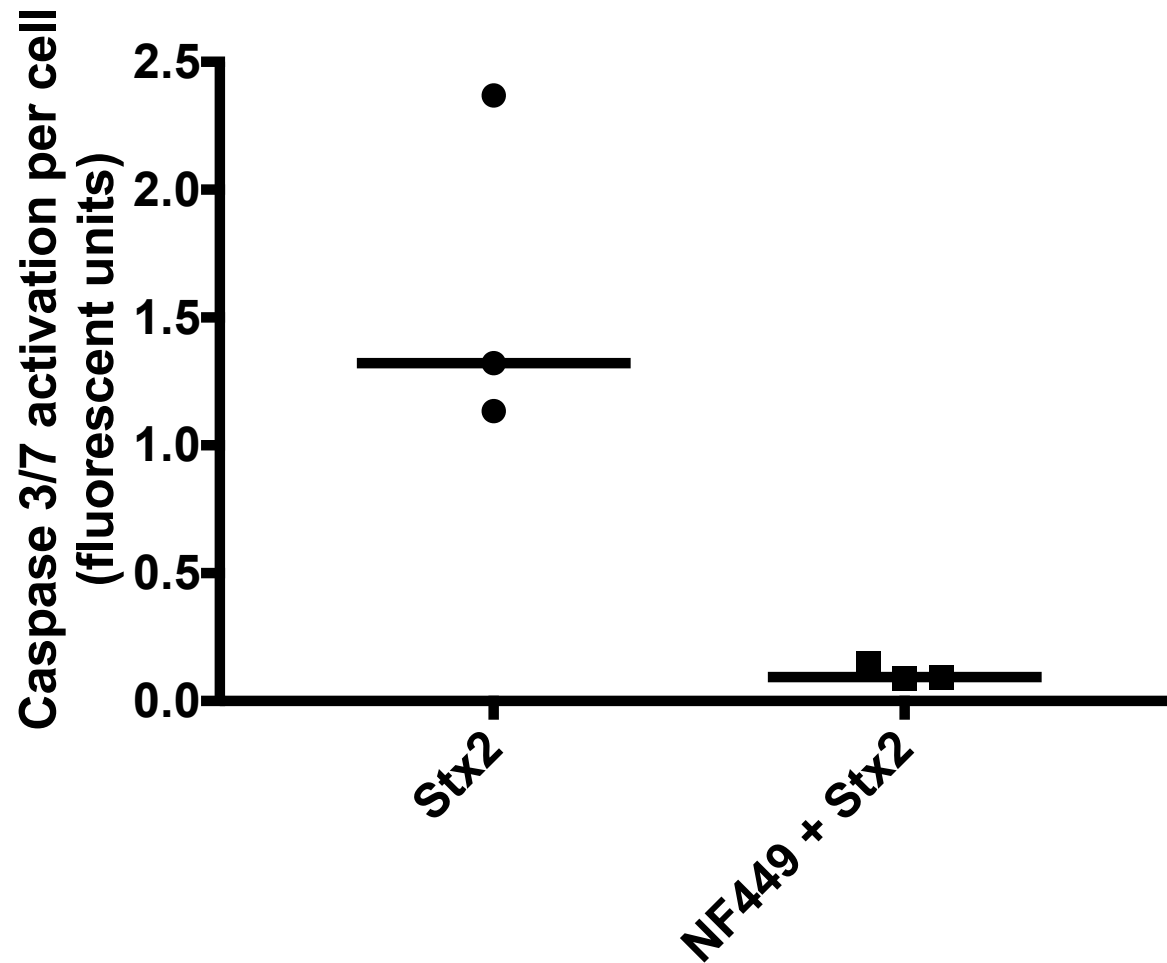


Figure S4: P2X1 blockade inhibits Stx2-induced apoptosis on HeLa cells

Shiga toxin 2 (Stx2)-induced caspase 3/7 activation was measured in HeLa cells pretreated with NF449 or left untreated, showing less caspase 3/7 activation in the cells that were pretreated with NF449. Data is presented as median caspase 3/7 activation per cell. The median is denoted by the bar.

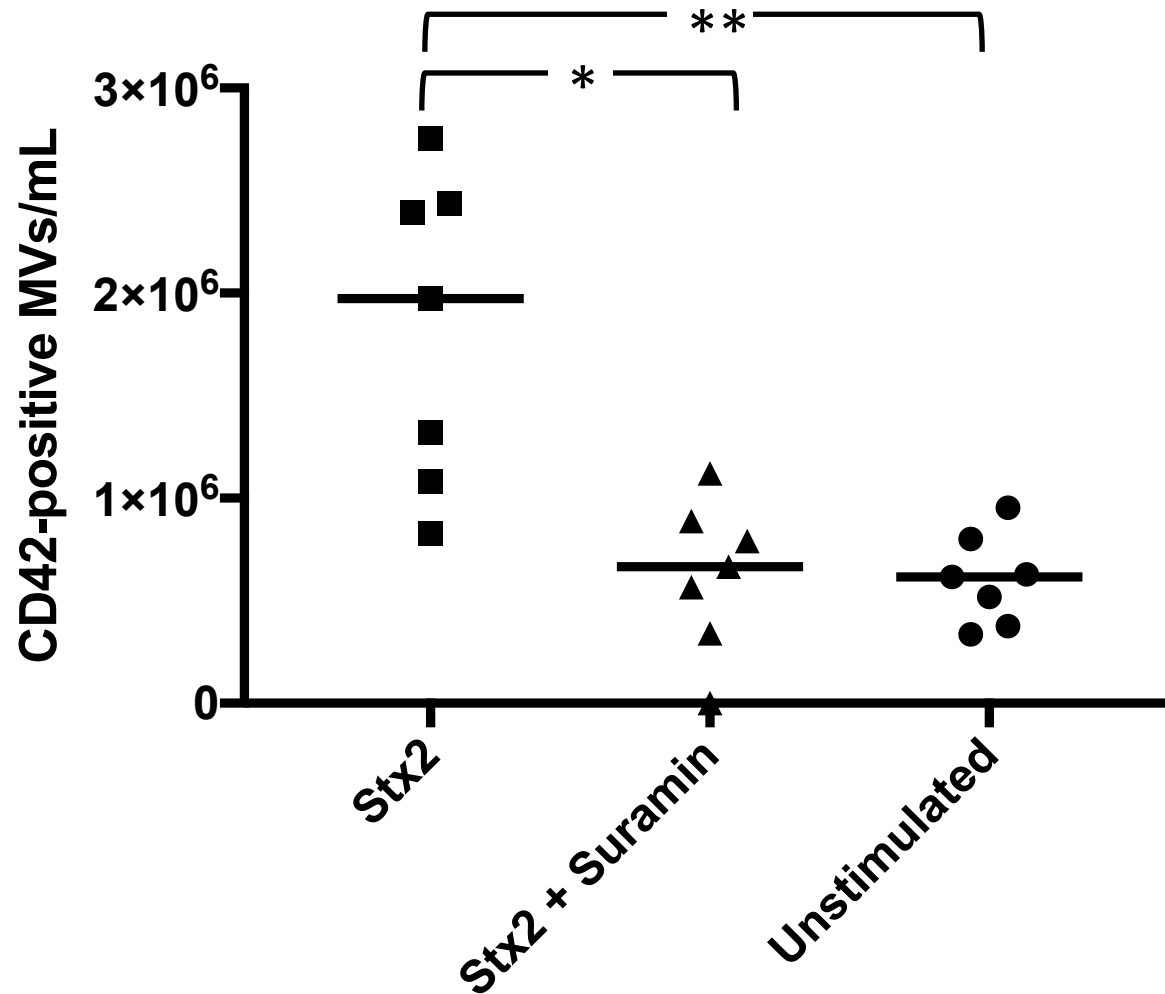


Figure S5: Suramin inhibits the release of platelet-derived microvesicles

Whole blood was pretreated with suramin or left untreated and stimulated with Shiga toxin 2 (Stx2). Stx2 induced a significant release of platelet-derived (CD42) microvesicles (MV) that was reduced by suramin (median MVs in the unstimulated control was 6.2×10^5 /mL). Data is presented as median MVs/mL. The median is denoted by the bar. *: $P < 0.05$, **: $P < 0.01$, Kruskal-Wallis test.

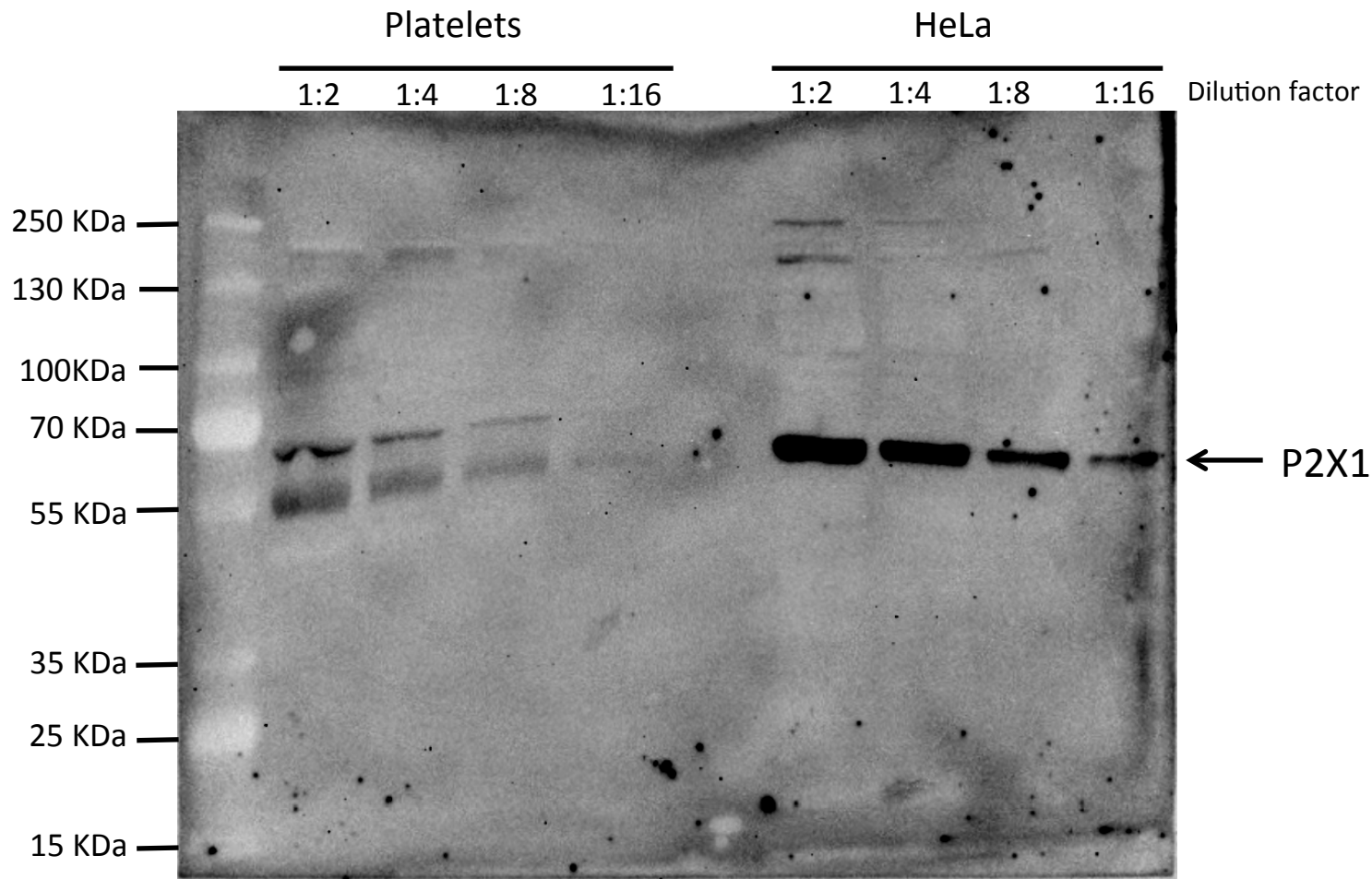


Figure S6: P2X1R in HeLa cells and platelets

HeLa cell and platelet lysates were separated by gel electrophoresis, transferred to nitrocellulose membranes and stained with an anti-P2X1 receptor antibody. Bands were detected by immunoblotting corresponding to approximately 60 kDa which is the size reported for P2X1.

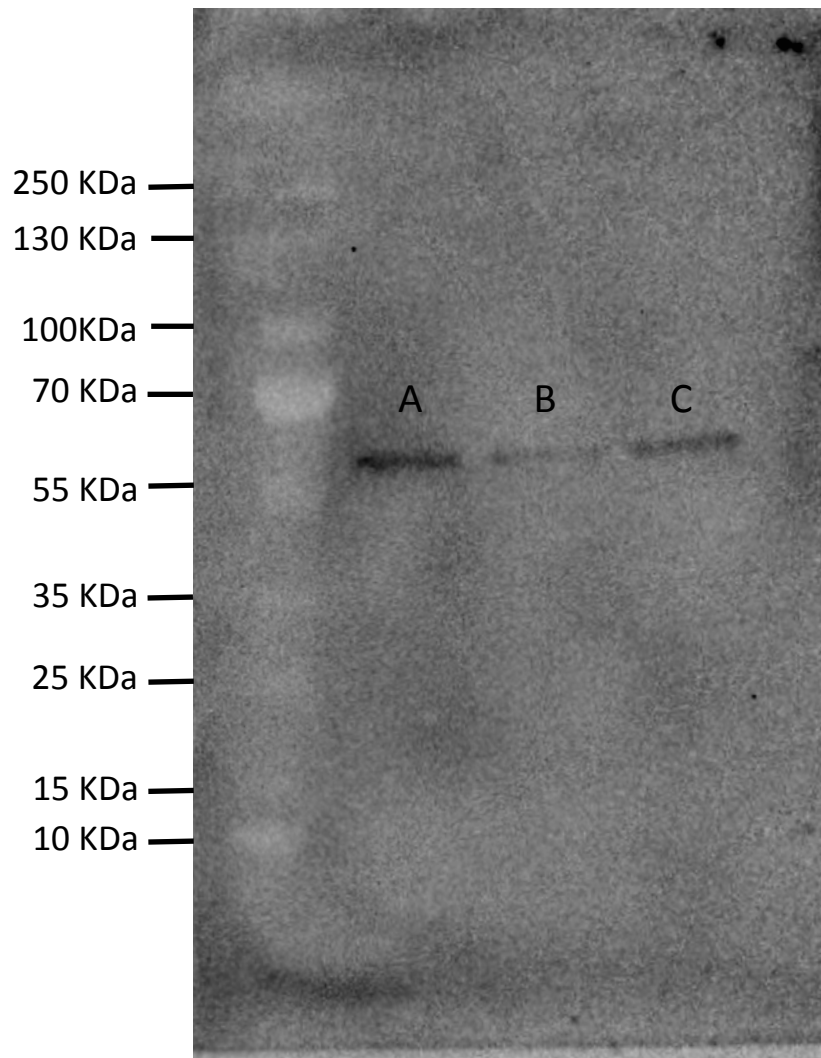


Figure S7: Silencing of P2X1 in HeLa cells

HeLa cells treated with (A) non-targeting control siRNA (siCtrl, 6 μ M) (B) siRNA targeting P2X1 mRNA (siP2X1, 6 μ M) or (C) siP2X1 (3 μ M) were lysed and protein content was separated by electrophoresis. P2X1 content was detected by immunoblotting as before. Bands were detected at approximately 60 kDa, corresponding to P2X1.

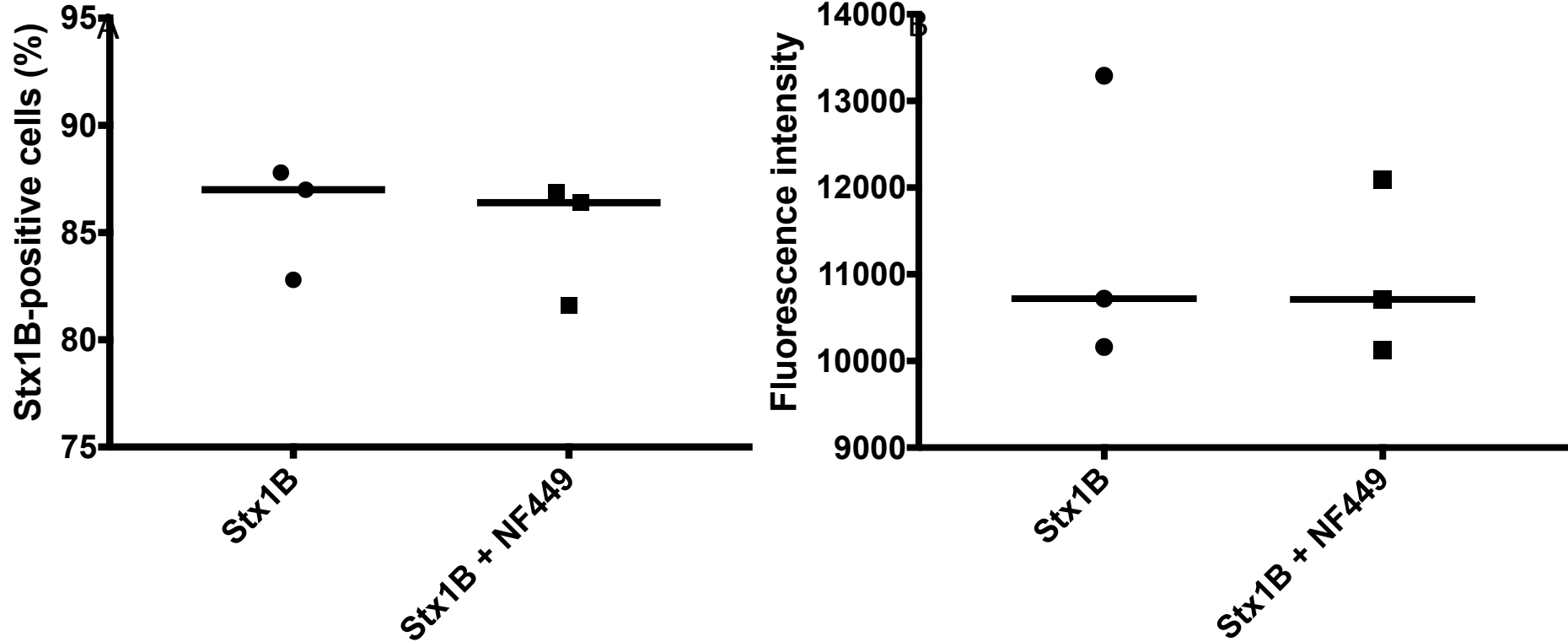


Figure S8: The effect of NF449 on Shiga toxin 1B-binding to HeLa cells

HeLa cells were pretreated with or without NF449 and incubated with Shiga toxin 1B (Stx1B). (A) Cells were analyzed by flow cytometry for the detection of Stx1B-positive cells, showing no statistical difference between NF449-treated and untreated cells. (B) The mean fluorescent intensity was measured, showing no statistical difference regarding Stx1B-positivity between untreated and NF449 treated cells. The bar denotes median percentage of Stx1B-positive cells or fluorescence intensity.

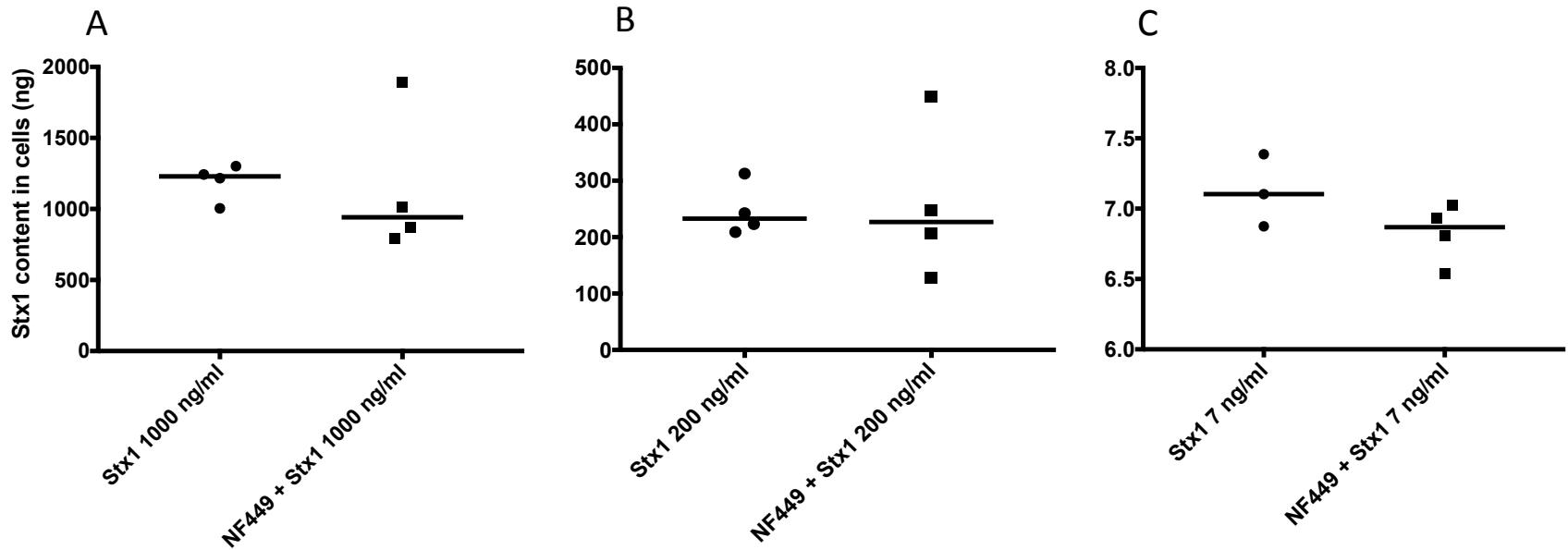


Figure S9: The effect of NF449 on Shiga toxin 1-uptake in HeLa cells

HeLa cells pre-treated with NF449 or PBS vehicle were incubated with Shiga toxin 1 (Stx1) at varying concentrations: (A) 1000, (B) 200 or (C) 7 ng/mL. Results showed that NF449 did not significantly alter the cellular uptake of Stx1. The median is depicted by the bar.